Facile Preparation of Magnetic Porous Carbon Composites from Sugarcane Bagasse via Simultaneous Magnetization and Activation and Their Use in Adsorption

Sirinad Mahawong

A Thesis Submitted in Partial Fulfillment of the Requirements for the Degree of Master of Science in Chemistry (International program)
Prince of Songkla University
2019

Facile Preparation of Magnetic Porous Carbon Composites from Sugarcane Bagasse via Simultaneous Magnetization and Activation and Their Use in Adsorption

Sirinad Mahawong

A Thesis Submitted in Partial Fulfillment of the Requirements for the Degree of Master of Science in Chemistry (International program)
Prince of Songkla University
2019

Thesis Title	Facile preparation of magnetic porous carbon composites from sugarcane bagasse via simultaneous magnetization and activation and their use in adsorption
Author	Miss Sirinad Mahawong
Major Program	Chemistry (International Program)

Major Advisor

.....

(Dr. Laemthong Chuenchom)

Examining Committee:

.....Chairperson

(Dr. Decha Dechtrirat)

.....Committee

(Assoc. Prof. Dr. Pongsaton Amornpitoksuk)

.....Committee

(Asst. Prof. Dr. Uraiwan Sirimahachai)

.....Committee

(Dr. Laemthong Chuenchom)

The Graduate School, Prince of Songkla University, has approved this thesis as Partial fulfillment of the requirements for the Master of Science Degree in Chemistry (International Program).

.....

(Assoc.Prof.Dr. Teerapon Srichana)

Dean of Graduate School

This is to certify that the work here submitted is the result of the candidate's own investigations. Due acknowledgement has been made of any assistance received.

.....Signature
(Dr. Laemthong Chuenchom)
Major Advisor

.....Signature
(Miss Sirinad Mahawong)
Candidate

I hereby certify that this work has not been accepted in substance for any degree, and is not being currently submitted in candidature for any degree.

.....Signature

(Miss Sirinad Mahawong)

Candidate

ชื่อวิทยานิพนธ์ การเตรียมวัสดุคาร์บอนที่มีรูพรุนและมีสมบัติแม่เหล็กจากชานอ้อย โดยวิธีการทำให้เป็นแม่เหล็ก และกระบวนการกระตุ้นพร้อมกัน เพื่อใช้ในการดูดซับ
ผู้เขียน นางสาวศิรินาถ มหาวงศ์
สาขาวิชา เคมี (หลักสูตรนานาชาติ)
ปีการศึกษา 2561

บทคัดย่อ

เตตราไซคลีน (Tetracycline, TC) เป็นหนึ่งในยาปฏิชีวนะที่มีการนำไปใช้มากที่สุดในประเทศไทย การปนเปื้อนของเตตราไซคลีนในแหล่งน้ำธรรมชาติก่อให้เกิดผลกระทบอย่างมากต่อสิ่งมีชีวิตและสภาพแวดล้อม ดังนั้นจึงมีความจำเป็นที่จะต้องหาวิธีเพื่อกำจัดสารปนเปื้อนชนิดนี้ ปัจจุบันกระบวนการดูดซับเป็นกระบวนการหนึ่งที่มีประสิทธิภาพสูงและมีการใช้อย่างแพร่หลายเพื่อกำจัดสารปนเปื้อนในแหล่งน้ำ ในงานวิจัยนี้จึงได้ทำการเตรียมวัสดุคาร์บอนที่มีรูพรุนจากวัสดุชานอ้อย อันเป็นสารชีวมวลจากอุตสาหกรรมผลิตน้ำตาล ด้วยวิธีการทำให้เป็นแม่เหล็กและกระบวนการกระตุ้นพร้อมกันในขั้นตอนเดียว เพื่อใช้ในการดูดซับ ในงานวิจัยนี้ได้ทำการศึกษาลักษณะทางกายภาพและทางเคมีของวัสดุคาร์บอนที่มีรูพรุนที่ได้จากการสังเคราะห์ด้วยเทคนิคหลากหลายประเภท พร้อมทั้งศึกษาปัจจัยที่ส่งผลต่อคุณสมบัติการดูดซับเตรตราไซคลีนของวัสดุคาร์บอน จากการศึกษาพบว่าวัสดุคาร์บอนที่สังเคราะห์ได้มีคุณสมบัติความเป็นแม่เหล็กที่มีประสิทธิภาพ มีความเสถียรภาพทั้งก่อนและหลังทำการดูดซับ และสามารถดูดซับเตตราไซคลีนได้สูงสุดถึง 48.40 mg/g จากข้อมูลสามารถอธิบายกลไกการดูดซับของวัสดุคาร์บอนด้วย **π-π** interactions ระหว่าง aromatic บนผิวหน้าของถ่านและเตตราไซคลีน การศึกษาพื้นที่ผิวด้วย BET surface พบว่ามีค่าสูงถึง 566 m^2/g และยืนยันการมีอยู่ของรูพรุนขนาดกลางมากกว่า 84 % ซึ่งมีความเหมาะสมในการดูดซับเตตราไซคลีน ดังนั้นจากการศึกษางานวิจัยนี้พบว่าวัสดุคาร์บอนที่มีรูพรุนและมีคุณสมบัติความเป็นแม่เหล็กจากชานอ้อยสามารถนำมาประยุกต์ใช้เพื่อกำจัดเตตราไซคลีนได้อย่างมีประสิทธิภาพ

Thesis Title	Facile preparation of magnetic porous carbon composites from sugarcane bagasse via simultaneous magnetization and activation and their use in adsorption
Author	Miss Sirinad Mahawong
Major program	Chemistry (International program)
Academic Year	2018

ABSTRACT

Tetracycline (TC) is one of the medicinal antibiotics most applied for people and veterinary usage in Thailand. The release of TC is speculated an intimidation to the water environment; hence, it immediately requires to be proficiently removed from the watercourse. One of the most popular and effective methods of removal of TC is adsorption. Magnetic carbon composites derived from biomass-based materials have attracted attention as novel adsorbents for removal of toxic substances from aqueous solution. However, their preparation involves multi-step procedures, which is time and energy consuming. In this work, we have prepared novel magnetic carbon composites using sugarcane bagasse, abundantly wasted biomass from sugar industries, a mixture of Fe^{2+} and Fe^{3+}, and NaOH, as a carbon precursor, source of magnetite particles (Fe_3O_4), and precipitating/activating agent, respectively. The facile preparation has been performed via a simultaneous magnetization and process in a single step. The effects of preparation conditions on physicochemical properties of the resulting materials were studied, discussed and optimized. A selected sample showed satisfactory magnetic stability due to the presence of Fe_3O_4 particles (confirmed by XRD) and high porosity, with a BET surface of 566 m^2/g and mesopore fraction (pore size > 2 nm) of more than 84%, suitable to adsorb the large TC molecules. The adsorption performance towards TC was determined using batch adsorption experiments. The maximum TC adsorption on the selected sample was as high as 48.40 mg/g, outperforming many literature sorbents, while the magnetic stability can even be retained after complete adsorption.

ACKNOWLEDGEMENTS

The achievement of my thesis would be impossible without the assistance of everyone. I wish to illuminate my appreciation to those who have contributed to the achievement of my thesis:

I wish like to express my deep gratitude to Dr. Laemthong Cheunchom, my research advisors, who has suggested this research problem, for his professional enthusiastic encouragement of this thesis during the development of this research work and the preparation of this thesis

I would like to express my very great appreciation to Assoc. Prof. Dr. Pongsaton Amornpitoksuk and my grateful thanks are also extended to Asst. Prof. Dr. Uraiwan Sirimahachai, who have given their times in criticizing the manuscript and suggested constructive recommendations for improvement of this research project, to Dr. Decha Dechtrirat, the examining chairperson for his great advice and improvement of this research thesis.

I am particularly grateful for Science Achievement Scholarship of Thailand (SAST) and also Center of Excellence for Innovation in Chemistry (PERCH-CIC) for their assistance and financial supports.

I wish to thank all staffs of the Department of Chemistry, Faculty of Science, Prince of Songkla University for their support in the equipment.

I wish to thank various people for their contribution, especially my lab members in Ch314 room for the motivation, enthusiastic encouragement and kindness during my research work and also my course works.

Finally, Special thanks should be given to my beloved family and friends for their support throughout my thesis work and also my study.

Sirinad Mahawong

THE RELEVANCE OF THE RESEARCH WORK TO THAILAND

Sugarcane bagasse is residue from sugar manufacturing processes from sugar cane. Sugar industry is one of the most important agricultural-produce processing industries for developing countries such Thailand. In Thailand, numerous amounts of sugarcane bagasse are produced every day from the sugarcane industry. A key issue to deal with this sugarcane bagasse waste is to find a suitable utilization of this solid waste. Sugarcane bagasse seems to be a great starting precursor for many applications because it contains suitable physical and chemical structures. There are few reports on the application of sugarcane bagasse.

In this work, we have focused on the development of a magnetic carbon adsorbent fabrication via simultaneous magnetization and activation process in a single process. Sugarcane bagasse, as an abundance carbon source, has been selected as a carbon precursor. Furthermore, Fe^{2+} and Fe^{3+} ions as a source of magnetic particles in the carbon adsorbent. NaOH is employed as both activating agent to develop the porosity and precipitating agent for the magnetite iron oxide (Fe_3O_4) particles. Subsequently, efficient, inexpensive and uncomplicated TC removal process was presented using the magnetic carbon composites synthesized in our work as adsorbents.

CONTENTS

Page

LIST OF FIGURES

Figure **Page**

LIST OF TABLES

Table **Page**

CHAPTER 1
INTRODUCTION

1.1 Introduction

The comprehensive application of antibiotics in livestock industries and humans has persuaded massive attention due to contrary impacts for human health and aquatic environment (Qiao et al., 2018). Therein, tetracycline (TC) (its chemical structure represented in Figure 1), a category on broad spectrum antibiotics (Chen et al., 2016), has popularly been employed. Furthermore, it has abundantly been accumulated in aquatic surroundings and soil, motivating chronic toxicity antibiotic defiance in microorganisms (Dong et al., 2018, Xie et al., 2016). For this reason, requirements to remove TC from aquatic systems before its further spread into soil are highly desirable. Various processes have been employed to eradicate this antibiotic, for example bio-degradation (Liao et al., 2016), photocatalytic degradation (Lofrano et al., 2016), oxidation, and adsorption (Gadipelly et al., 2014). In sight of environmental discretions and economics, adsorption has been considered as an energetic technique. However, most of adsorbent materials currently applied nowadays encounter the problems of multiple-step manufacturing processes, leading to total high-costs for the industrial scale production.

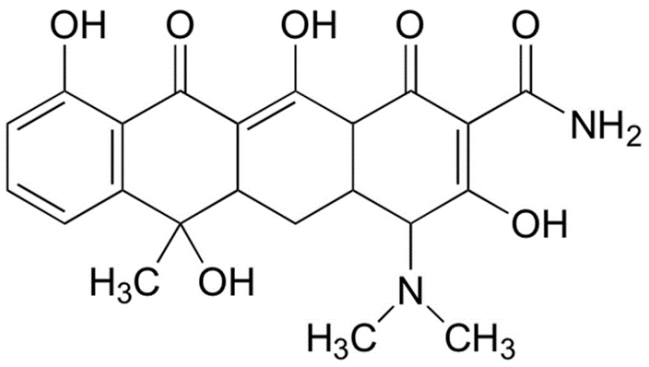

Figure 1. Chemical structure of tetracycline (TC) (Gao et al., 2012)

Recently, magnetic carbon adsorbents have brought out huge attentions on divergent fields because of their exclusive magnetic properties, pore volume and large specific surface area (Kim et al., 2008, Zhou et al., 2015, Zhou et al., 2014, Rai and Singh, 2018). Therefore, these types of magnetic adsorbents are attractive in removing several environmental pollutants for example organic dyes, antibiotics and heavy metal ions as well (Mehta et al., 2015). Graphene oxide functionalized magnetic particles (GO-MPs) was fabricated for tetracycline removal in water remediation (Lin et al., 2013b). The maximum adsorption capacity of this magnetic composites illustrated approximately 39.1 mg/g for TC adsorption. Magnetic cellulose/Fe_3O_4/activated carbon composite (m-Cell/Fe_3O_4/ACCs) presented the efficacy adsorption for congo red (Zhu et al., 2011). Both appropriate separation method and great efficiency encourage m-Cell/Fe_3O_4/ACCs as one of the attractive magnetic adsorbents. Despite a great recoverability of the abovementioned materials, the starting precursors were non-renewable and costly, which strongly limits their large scale productions (Hao et al., 2014, Cazetta et al., 2016).

Sugarcane bagasse is residue from sugar manufacturing processes, which is the major industry in several countries such as China, Brazil, Thailand and Mexico, etc. In Thailand, numerous amounts of sugarcane bagasse are produced every day from the sugarcane industry. A key issue to deal with this sugarcane bagasse waste is to find a suitable utilization of this solid waste. Sugarcane bagasse seems to be a great starting precursor for many applications because it contains suitable physical and chemical structures (Pandey et al., 2000). Department of Agricultural Extension in Thailand reported that Thailand produced almost 30 million tons of sugarcane bagasse in each year (Laopaiboon et al., 2010). For this reason, finding alternative, innovative and sustainable routes in utilizing such sugarcane bagasse waste can lead to the production of added-values chemicals and/or functional materials.

For this task, we have focused on the development of a magnetic carbon adsorbent fabrication via simultaneous magnetization and activation process in a single process. Sugarcane bagasse, as an abundance carbon source, has been selected as a carbon precursor. Furthermore, Fe^{2+} and Fe^{3+} ions as a source of magnetic particles in the carbon adsorbent. NaOH is employed as both activating agent to develop the

porosity and precipitating agent for the magnetite iron oxide (Fe_3O_4) particles. Subsequently, efficient, inexpensive and uncomplicated TC removal process was presented using the magnetic carbon composites synthesized in our work as adsorbents. The magnetic carbon composites prepared here show good magnetic stability and high adsorption efficiency towards TC. Furthermore, by systematic investigating the effect of NaOH concentration, our findings state the importance of the impact of mesoporosity on the improvement of adsorption toward TC.

1.2 Preliminary knowledge and Theoretical section

1.2.1 Definition of porous carbon

The porous carbon is the carbons with porosity which the pores are straggled over a high range of carbon shape and size as well. Furthermore, the classification of pore size can be categorized via the size of pores normally into 3 types: (i) maccropores (diameter >50 nanometers), (ii) mesopores (diameter 2–50 nanometers), and (iii) micropores (diameter <2 nanometers). In addition, the porous carbons are farther differentiate into supermicropores (diameter 0.7–2.0 nanometers) and ultramicropores (diameter <0.7 nanometers).

These carbons also can be group into 2 types which are (i) Activated carbons with added chemical groups and (ii) Carbon foams.

The activated carbon is a carbonaceous which is the one of special kind of carbons for industrial and also have been applied for several years. In addition, this carbon apply in aqueous purification for medicinal purposes.

The newest addition of porous carbons is activated carbon fibres. These materials have added add the potential to energy areas and gas storage.

In the figure 2, the wood derived carbons show the existence of pore structure which is a remembrance for the texture of the precursor. Thus, the difference kind of woods illustrate the difference texture.

Normally, these porous carbon derived from plant consist of macropores as well as slit-like voids. In some plants for example pine, they have analogous form and size. Moreover, they have equally distributed, whereas in bagasse, castor oil wood and so on the pores are quite different characteristics.

In figure 3 illustrates the characteristic of activated carbon fibers. In the contrary with wood-based activated carbon, obviously consist of micro porous structure certainly exposed to the fibered surface.

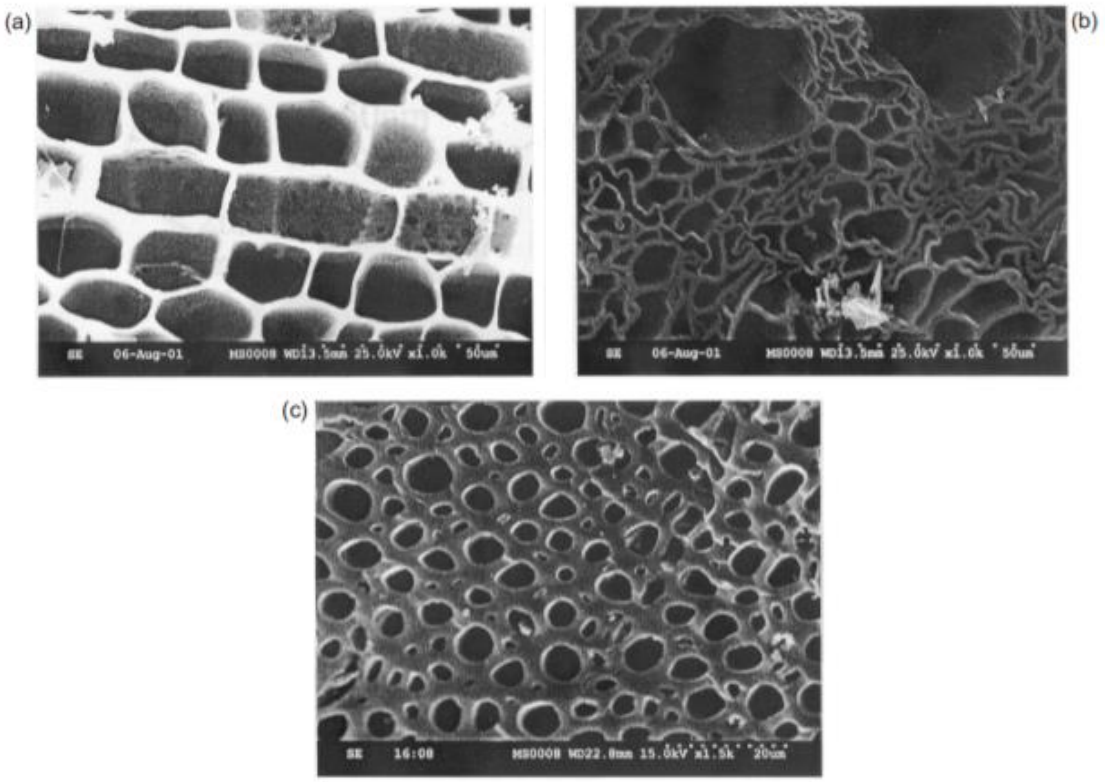

Figure 2. SEM micrographs of porous carbons:
(a) castor oil plant wood and (b) bagasse (c) babbool wood (Manocha, 2003).

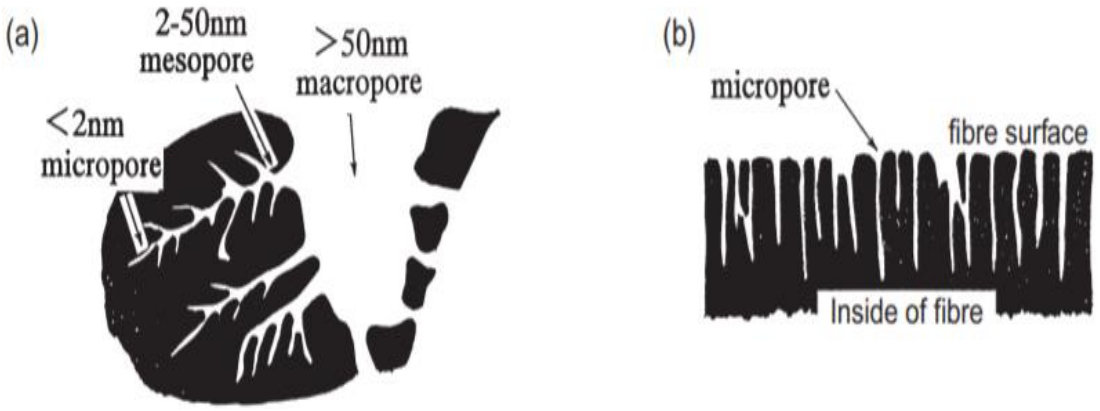

Figure 3. Pore structure of activated carbon: (a) granular and (b) fibrous (Manocha, 2003).

1.2.2 Carbonization process

In the carbonization technique, from the pyrolytic decomposition of the starting materials, the first removed in gaseous are H_2, O_2 and also non-carbon elements. Moreover, the graphite crystallites are grouped from the elementary carbon (free atom form). Therefore the carbonization relates to the disposing of non-carbon species creating a fixed carbon mass as well as pore structure and thermal decomposition in carbonaceous material.

The important parameters in carbonization process determine the yield and also the quality of the carbonaceous product that the method is always proceeded at temperature below 800 ˚C in an inert atmosphere. There are several parameters that effect to the yield of product and also the quality of the carbonaceous material such as soaking time, final temperature and rate of heating.

In addition, at around 500 ˚C during the pyrolysis, the micropores are generated but some of these are blocked. Farther heat treatment process to around 800 ˚C is given, the microstructure of char with microporosity could be obtainable. Moreover, when farther heat treatment to around 1000 ˚C is given, the carbon structure lead to hardening and decrease in porosity which accelerate the activation (Manocha, 2003).

1.2.3 Activation

Principally, depending on the degree of crystallographic ordering, the carbons are classified to non-graphitic and graphitic. The non-graphitic carbon possess two-dimensional of carbon atom while graphitic carbons have three-dimensional of carbon atom (Zhu et al., 2013, Xie et al., 2019, Sankar et al., 2019).

As mentioned above, the deposition of tar is the cause of blocked micropore. Thus, the resulting materials illustrate a pretty small amount of adsorption capacity. Possibly, the carbonized materials can be activated by heating under inert atmosphere such as N_2 for eliminating the tar.

Therefore, the activation process is accomplished to enhance the pore size which is established in the carbonization method. Furthermore, to establish microporosity as resulting in both creation of a well-developed and also accessible pore structure with very high internal surface area (Manocha, 2003).

1.2.4 Classification of activated carbon

Activated carbon is complicated product that is hardy to categorize on the rudiment of its preparation method, behavior as well as surface characteristics. Nevertheless, some broad categories is establish for regular target based on its physical characteristics (Oubagaranadin and Murthy, 2011, Manocha, 2003).

(1) Powdered activated carbon (PAC):

Normally, the active carbons are produced in specific design for example fine granules or find powders lower than 100 mm in size. So they must show a huge internal surface with a low diffusion distance (Lompe et al., 2018, Manocha, 2003).

(2) Granulated activated carbon (GAC):

Granular activated carbon illustrates a relatively higher particle size compared with PAC and accordingly, represent a miner exterior surface. Therefore, an essential factor is the adsorbate diffusion. The Granular activated carbons are preferred for adsorption of vapours and also gases as their rate of diffusion are faster. The granular activated carbons are applied for separation of components of flow system and deodorization as well as water treatment (Dwivedi et al., 2018, Manocha, 2003, Tao et al., 2017).

(3) Spherical activated carbon (SAC):

Spherical activated carbons (SACs) are created by tiny spherical balls therein pitch is melted in the owning of tetorlin or naphthalene and then changed into spheres. The SACs are implicated with solution naphtha, that separates naphthalene as well as establish the porous structure. Then, The porous structure are treated at high temperatures from 100 ˚C to 500 ˚C in the existence of an oxidizing gas filling as 40% of O_2 by weight. Then, the oxidized spheres are heated from 160 ˚C to 700 ˚C in the existence of NH_3 to approach N_2 into spheres that is then activated in carbon dioxide or steam. The spherical activated carbons show very good NO_2 as well as SO_2 adsorption efficiency. Furthermore, they possess huge mechanical strength (Ouzzine et al., 2019, Manocha, 2003, Sankar et al., 2019).

(4) Impregnated carbon:

Porous carbon materials consisting various kinds of inorganic impregnant for example I, Ag as well as cation have been made for particular application in air pollution control particularly in museums and galleries. The activated carbons loaded by Ag are employed for adsorb the pollution in water environment. In addition, the natural water can be generated water for drinking by natural treatment and also a mixture of activated carbon with $Al(OH)_3$ as a flocculating. This carbon is applied for the mercaptans (thiols) as well as the adsorption of H_2S (Li et al., 2019, Manocha, 2003, Jin et al., 2016).

(5) Polymers coated carbon:

Polymers coated carbon is the porous carbon can be coated with a biocompatible polymer to provide a penetrable coat and give the smooth with no blocking pores. Interestingly, this porous carbon is normally used in hemoperfusion (Manocha, 2003).

1.2.5 Adsorption by activated carbons

Adsorption is the adhesion of molecules, ions or atoms from liquid or gas to a surface and formation of a liquid layer or gaseous layer by molecules on surface of a solid from molecular attraction of the van der Waals force which are weak forces (Kong and Adidharma, 2019, Zhu et al., 2013). The atoms on the solid face such active carbons possess inequitable forces as compared to those within the solids. The adsorbates establish a monolayer on the surface of adsorbent (Manocha, 2003).

The activated carbons as adsorbent adsorb the adsorbed molecules by using the specific surface area and pores as well. Furthermore, it's a dynamic method in which some adsorbate molecules are released to the liquid or gaseous state although some are converted from the liquid or gaseous phase on to the adsorbent surface. In which these procedures are functions of partial pressures.

Whenever the speed for 2 procedures is equal, the equilibrium of adsorption process or ostensible adsorption isotherm is achieved. This illuminate the quantity of liquid or gaseous molecules adsorbed such as a function of gas phase concentration determine by equilibrium partial pressure p/p_o at constant temperature. In addition, the adsorption capacity can be called in term adsorption isotherm is used to predict pore volume in many porosity regimen, surface area, evaluation of the surface chemistry about the adsorbent as well as essential data on the proficiency of industrial carbon hired in purification process and separation method.

Figure 4 portrays the method in adsorption indicating migrate of the molecules pass through the bulk gas phase to the surface of the adsorbent and diffusion into the inner surfaces of the pores in the adsorbent.

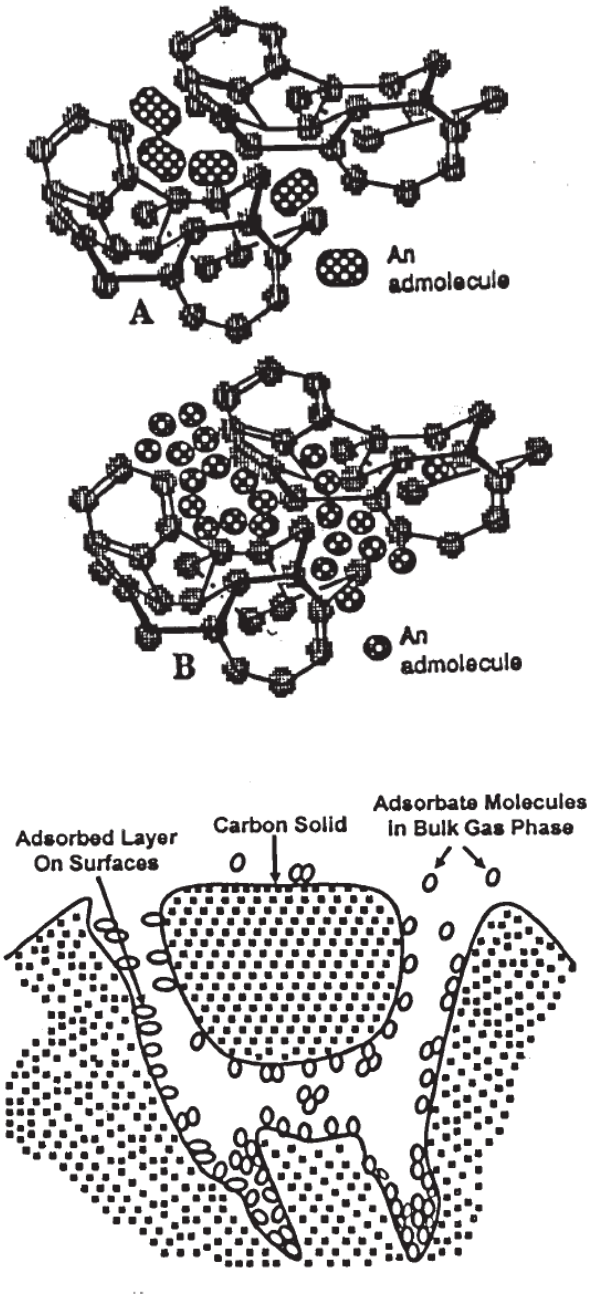

Figure 4. Adsorption processes in activated carbons:
Transfer of adsorbate molecules to adsorbent (Manocha, 2003).

For Basically, the kind of attraction forces in adsorption procedure between adsorbent (solid) and adsorbate (liquid) can be separated into 2 types: (i) chemical adsorption and (ii) physical adsorption (Wang et al., 2019, Braghiroli et al., 2019). The process that removes the molecule from surface is called desorption.

(1) Chemisorption

Chemisorption is occurred between the surface of adsorbent and the adsorbate by direct chemical bonding with monolayer formation. The chemical bonding cannot be broken by only enlarged temperature. The chemisorption has high enthalpy for adsorption and it is always irreversible procedure.

(2) Physisorption

Physisorption is occurred when the adsobate molecules were held by physical forces such as Van der Waals force with the multilayer formation between adsorbate and adsorbate. In addition, this force can be removed when increasing temperature (by remove the molecule from surface). Hence, physisorption has low enthalpy for adsorption and it is usually reversible procedure (Manocha, 2003).

Comparison between Physisorption and Chemisorption

Physisorption	Chemisorption
1. Low heat of adsorption usually in the range of 20-40 kJ mol^{-1}	High heat of adsorption in the range of 40-400 kJ mol^{-1}
2. Force of attraction are Van der Waal's forces	Forces of attraction are chemical bond forces
3. It usually takes place at low temperature and decreases with increasing temperature	It takes place at high temperature
4. It is reversible	It is irreversible
5. It is related to the ease of liquefaction of the gas	The extent of adsorption is generally not related to liquefaction of the gas
6. It is not very specific	It is highly specific
7. It forms multi-molecular layers	It forms monomolecular layers
8. It does not require any activation energy	It requires activation energy

1.2.5.1 Adsorption kinetics

(1) Pseudo first order

A Pseudo first order equation can be explained the adsorption kinetics for solid and liquid phase adsorption. This equation is believed to be the earliest model for measuring the rate for adsorption. This equation can be represented as follows:

$$\frac{dq_t}{t} = k_1(q_e - q_t) \quad (1)$$

q_t (mg/g) is the adsorption capacity at time t (min).

q_e (mg/g) is the adsorption capacity at equilibrium.

k_1 (min^{-1}) is the pseudo-first-order rate constant.

Integrating Eq. (1) with the boundary conditions of $q_t = 0$ at t = 0 and $q_t = q_t$ at t = t, yields

$$\ln\left(\frac{q_e}{q_e - q_t}\right) = k_1 t \quad (2)$$

(2) Pseudo second order

In 1995, Ho explained a kinetic process of the adsorption of divalent metal ions onto peat. It can be represented as follows:

$$\frac{dq_t}{t} = k_2(q_e - q_t)^2 \quad (3)$$

Integrating Eq. (3) with the boundary conditions of $q_t = 0$ at t = 0 and $q_t = q_t$ at t = t, yields

$$\frac{t}{q_t} = \frac{t}{q_e} + \frac{1}{k_2 q_e^2} \quad (4)$$

1.2.5.2 Adsorption isotherm

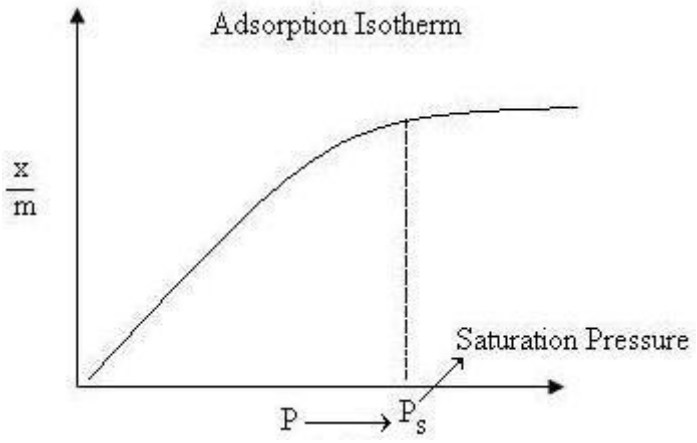

Figure 5. The basic adsorption isotherm. (Helfferich, 1985)

The adsorption technique known as adsorption isotherm or adsorption capacity is normally studied by graphs (Kumar Singh and Anil Kumar, 2018, Xie et al., 2019, Helfferich, 1985). The graphs present the number of adsorbed molecules towards adsorbent (solid) as concentration at constant temperature or a function of their pressure. The dosages of adsorbed molecules are practically normalized by the mass of the adsorbent (solid) to permit comparison of various materials.

As shown in Figure 5, predicting that the adsorption cannot occur anymore after Ps or saturation pressure. Possibility, this result can be described due to the fact that there are constrained by the number of vacancies of the adsorbent surface.

At the high pressure, almost all of the active sites are occupied and also farther add in pressure doesn't cause any divergence in adsorption procedure. This adsorption procedure is at an equilibrium point.

(1) Langmuir isotherm

Irving Langmuir represented a model isotherm for gases adsorbed to solids in 1916. This kind of isotherm generated from a proposed kinetic mechanism.(Helfferich, 1985).

$$A_{(g)} + B_{(s)} \xrightarrow{Adsorption} AB$$

Where $A_{(g)}$ is unadsorbed gaseous molecule.

$B_{(s)}$ is unoccupied adsorbent surface.

AB is Adsorbed gaseous molecule.

In this study of solid-liquid adsorption, the non-linear Langmuir adsorption isotherm is expressed in Eq. (5)

$$q_e = \frac{q_m b C_e}{1 + b C_e} \quad (5)$$

Where q_e(mg/g) is equilibrium adsorption capacity.

q_m(mg/g) is maximum adsorption capacity.

b is the Langmuir isotherm coefficient.

C_e is the equilibrium concentration of adsorbate.

In addition, linear form of this adsorption model which easier to fit the data. The linear equation is showed in Eq. (6).

$$\frac{C_e}{q_e} = \frac{1}{bq_e} + \frac{C_e}{q_m} \quad (6)$$

Assumption of Langmuir isotherm

Langmuir proposed his theory by making following assumptions (Helfferich, 1985).

1. The molecules (adsorbates) don't interact.
2. The all adsorption methods occur by the identical mechanism.
3. A monolayer is formed at the equilibrium.
4. The adsorption sites are impartial because the adsorbent surface is uniform.

Limitations of Langmuir isotherm

Langmuir Isotherm has the following limitations (Helfferich, 1985).

1. The real surface of solids are heterogeneous.
2. The Langmuir adsorption model assumed that the adsorbate molecules do not intetact with each other but it is impossible. Due to the weak force occurs although between the same type molecules.
3. The model assumed that adsorption is generated in monolayer. In the fact that monolayer creation is possible under low pressure only.
4. The adsorbed molecules has to be localized. This is not possible because on adsorption liquefaction of gases to taking place which results into decrease in randomness, but the value is not zero.

(2) Freundlich isotherm

Freundlich represented an empirical equation for indicating the isothermal variation of adsorption of a quantity of gas adsorbed by unit mass of solid adsorbent with pressure. The equation is known as Freundlich adsorption isotherm. Freundlich Adsorption Isotherm as shown in Eq. (7)

$$q_e = K_F\, C_e^{1/n} \tag{7}$$

Where q_e(mg/g) is equilibrium adsorption capacity.

C_e is the equilibrium concentration of adsorbate.

K_F is Freundlich adsorption constant.

n is adsorption intensity.

The linear form of Freundlich Adsorption Isotherm is usually used to fit data as:

$$log q_e = log K_F + \frac{1}{n} log C_e \tag{8}$$

1.2.6 Magnetite

Magnetite is a mineral that was discovered before the 4th century in China. It can naturally occur as well as in creatures such as bee, termite, some bacteria (*Aquaspirillum magnetotacticum*) and pigeon. The chemical formula of magnetite is Fe_3O_4. It has 2 crystal structures: spinel and inverse spinel. The spinel structure formula is AB_2O_4 consisting of A 1 atom in tetrahedral site and B 2 atoms in octahedral site whereas inverse spinel has A 1 atom and B 1 atom in octahedral site and B 1 atom in tetrahedral site as shown in Figure 1. The magnetite contains 1 atom of Fe^{2+} and 2 atoms of Fe^{3+}, thus A atom is Fe^{2+} being in octahedral site and B atom is Fe^{3+} being in both octahedral and tetrahedral site. This kind of arrangement leads to the delocalization of electron which is origin of magnetic properties of magnetite (E. Diebel et al., 2000, Lin et al., 2006).

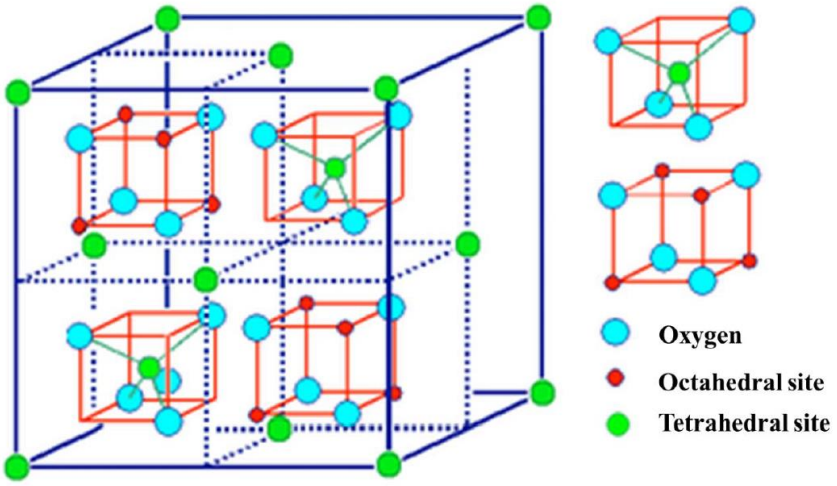

Figure 6. The inverse spinel structure of magnetite is shown indicating the tetrahedral and octahedral sites (Issa et al., 2013).

However, the magnetic properties of materials depend on their structure and electronic configuration which can be explained by quantum mechanics. This makes the magnetic spin of electron can be only up and down or can be called “magnetic dipole moment”.

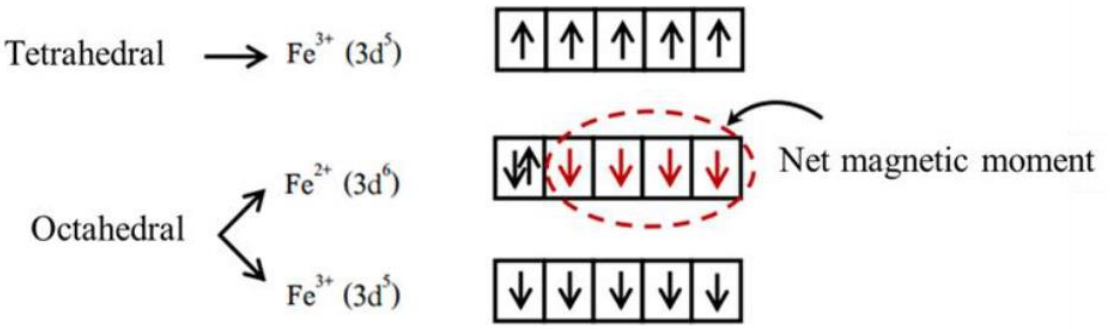

Figure 7. The spin configuration of electrons in the magnetite molecule (Issa et al., 2013).

When the number of electrons which has spin “up” are not equal to the number of electrons which has spin “down” resulting in the net magnetic dipole moment is not equal zero which rises magnetic properties in materials. To be noted

that, this state can happened only with paramagnetic materials (unpaired electron) (Issa et al., 2013).

Magnetite is the oldest known magnetic substance in group of ferromagnetic which means the spin of electron in octahedral and tetrahedral sites are opposite as shown in Figure 7. The 3d electrons of Fe^{3+} in both sites are equal and completely neutralized, but 3d electrons of Fe^{2+} aren't. They remain 4 unpaired electron with spin "down" in octahedral site causing the net magnetic dipole moment is not zero, thus the magnetite has magnetic properties.

In addition, if the size of magnetite is small enough to nanoparticles, the new behavior appears. It's so called "superparamagnetic". This superparamagnetic materials will randomly flip their spin of electrons in the absence of an external magnetic field which makes the materials has no residual magnetization. However, in the presence of external magnetic field, the magnetic moment is rearrangement to the direction of external magnetic field or can be said that they can be magnetized only in the external magnetic field as shown their behavior like hysteresis loop in Figure 8.

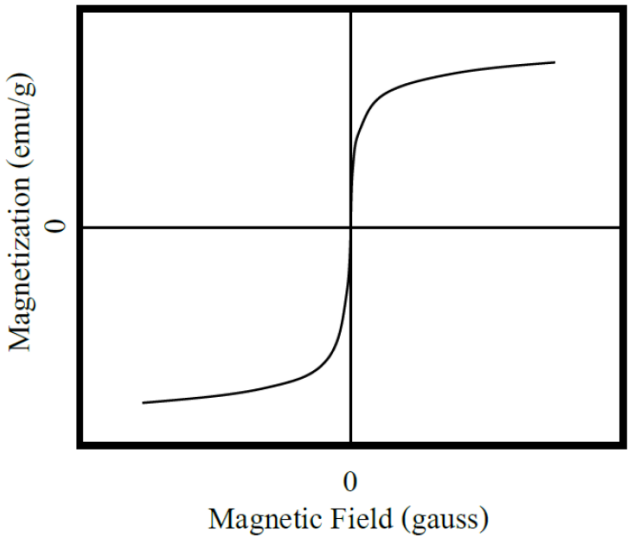

Figure 8. The hysteresis loop of superparamagnetic materials (Issa et al., 2013).

1.2.7 Tetracycline

Tetracyclines (TCs) or (4S,4aS,5aS,6S,12aR)-4-(dimethylamino)-1,6,10,11,12a-pentahydroxy-6-methyl-3,12-dioxo-4,4a,5,5a-tetrahydrotetracene-2-carboxamide with a molecular formula of $C_{22}H_{24}N_2O_8$ and molecular weight of tetracycline is 444.44 g/mol as shown its structure in Figure 1. TCs have many form in various pH conditions due to its amphoteric properties as shown in Figure 9 with their pKa values. Moreover, its size can be shown in Figure 10 which is very close in various pH.

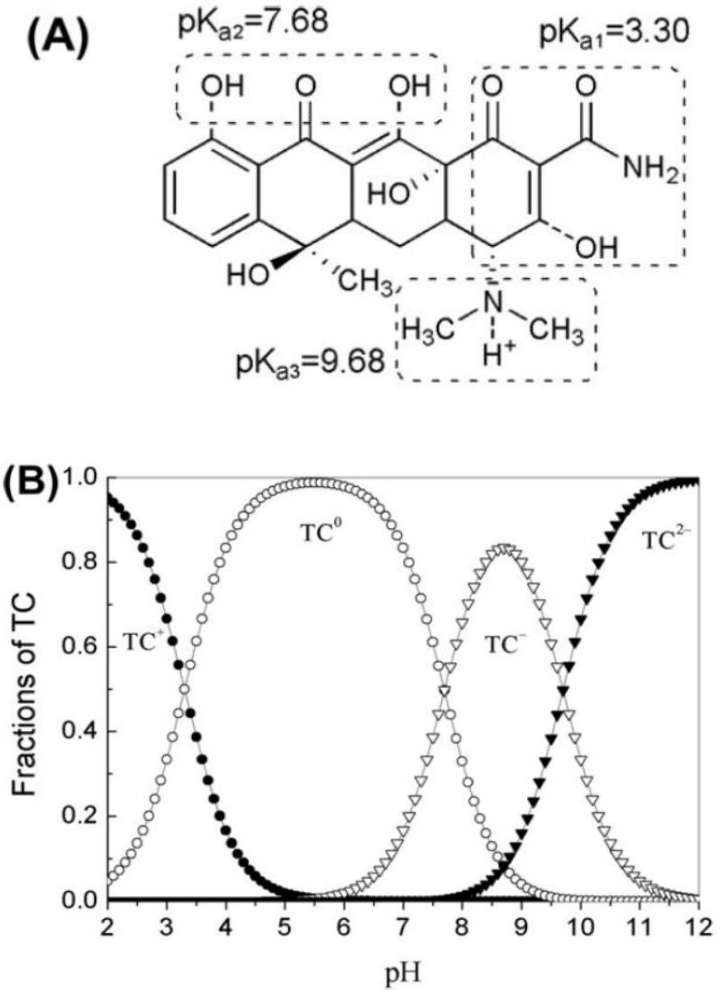

Figure 9. (A) Molecular structure of TC. (B) The fraction of cationic, neutral, and anionic forms of TC at different pH (Zhou et al., 2012).

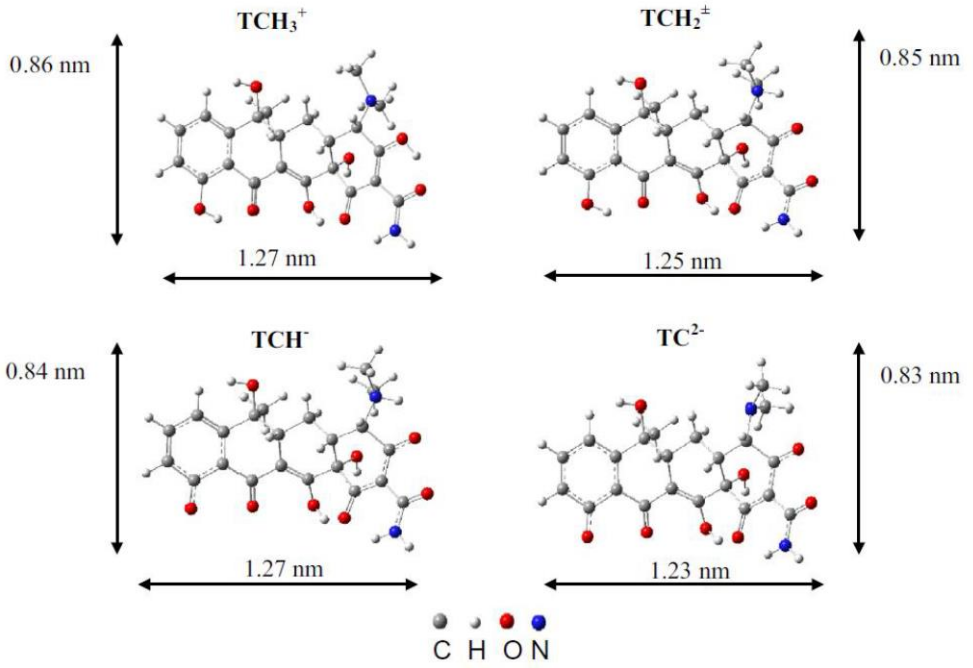

Figure 10. Molecular structures and sizes of TC species (Martins et al., 2015).

TCs are medicinal antibiotics, which are applied popularly use in human as well as agricultural. In addition, TCs have attracted gradually increasing consider in recent years, that TCs have been substantiated to be pollutants (Álvarez-Torrellas et al., 2016, Jing et al., 2014, Ma et al., 2014, Martins et al., 2015, Ou et al., 2016, Peng et al., 2014, Zhang et al., 2015) Because of they are badly metabolized and also absorbed by animals and humans, high fractions are defecated through urine and feces as unmodified parent compound. The leavings of TCs defecated from agricultural runoff and municipal wastewater treatment plants are frequently detected in soil and even surface water. The ubiquitous of TCs can potentially lead to long-term adverse consequences on various ecosystems, including severe and chronic toxicity and propagation of antibiotic resistance in microbes. Specifically, the tetracycline antibiotics also have been represented to break microbial soil respiration, Fe(III) reduction, nitrification, and phosphatase activities (Chang et al., 2012, Zhu et al., 2014b).

1.3 Review of literature

Lately, there are several researches about the application of biomass produced magnetic carbon materials as adsorbent. However, those resulting materials still use toxic chemical, high cost and also multi-step procedures. Some of those materials not only used multi-step procedures but also showed the low adsorption capacity.
such as:

Bastami and Entezari (2012) produced an activated carbon from carrot dross (AC) which is low cost and also facile to separate of solid phase from aqueous solution. Moreover, the resulting material represents the great property of adsorption from p-nitrophenol in aqueous solution. The carbonization procedure was carried out at 500 °C holding for 1 h in air condition before magnetizationm by using co-precipitation method. Remarkably, the adsorption were carried out in the presence and absence of ultrasonic irradiation in order to optimize stirring procedures. However, the adsorption efficiency decreased with the increasing of magnetite ratio on the surface of MAC. The maximum adsorption capacity (Q_{max}) of MAC was 85 mg/g with saturation magnetization of 4.47 emu/g (Bastami and Entezari, 2012).

Zhu and coworkers (2014) produced a new magnetic porous carbon (MPC) in one step with maghemite (γ-Fe_2O_3) from hydrochar (a solid residue of hydrothermal carbonization of biomass) through simultaneous activation and magnetization. The target in this work is remove tetracycline, one of the antibiotics by filling the hydrochar in $FeCl_3$. After that dried and pyrolyzed at 973 K for 1 h under nitrogen (N_2) flow. The resulting sample is a good carbon material as adsorbent for displacement of tetracycline. The enriched surface area of the magnetic porous carbon (MPC) and also its graphite-like structure, might encourage to the adsorption efficiency of tetracycline (Zhu et al., 2014a).

Zhu and coworkers (2008) have to synthesized magnetic porous carbon microspheres via the carbonization procedure with chitosan microspheres and iron precursors. By multi-proceduress such filling chitosan in acetic acid and toluene solution. Then, Crosslinking was carried out with glutaraldehyde, followed by Sodium hydroxide. Lastly, chitosan microspheres was accomplished. In addition, the magnetization procedure was done by using $(NH_4)_3[Fe(C_2O_4)_3]$ with the carbonization

procedure under Argon atmosphere at 700-1000°C for 4 h. The optimized temperature is at 1000°C which gave highest BET surface area. The synthesize sample show a porous structure with a very large surface area. Thus, the resulting sample can use to adsorb the nitrobenzene and also phenol in aqueous solution. Moreover, the microspheres represent the adsorption capacity as high as 35 mg/g and 97 mg/g, respectively. But the oftimized sample present the magnetization only 13.9 emu/g. Interestingly, the adsorbed molecules also can released in ethanol solution at ambient temperature. In addition, the synthesized microspheres were facile separated during the adsorption procedure and also the desorption procedure (Zhu et al., 2008).

Ma and coworkers (2015) was successfully produced a novel versatile magnetic adsorbent derived from corncob (MCA). By using the hydrothermal procedure and carbonization method at low temperature. The carbonized sample was mixed between iron (III) salt and NaOH for magnetization. The synthesize sample represented a porous structure with higher oxygen-containing than its carbon precursor (CP). The adsorption efficiency of both MCA sample and CP sample can be explained by pseudo-second-order model and also Langmuir isotherm. MCA sample shows the adsorption capacity with methylene blue as high as 163.93 mg/g while CP sample shows the lower adsorption capacity as high as 103.09 mg/g, due to its high surface area, porous structure as well as highly of active adsorption sites resulted from the catalytic effect of Fe (III) of MCA sample. Interestingly, The MCA sample was represented as a versatile adsorbent for both cationic and anionic dyes adsorption and facile to separate by an external magnet (Ma et al., 2015).

Kharissova and coworkers (2015) published reviews in the topic of Magnetic adsorbents based on micro- and nanostructured materials. They summarized the most recent achievements in the preparation and main applications of magnetic adsorbents, focusing mainly on nano- and micro-sized magnetic particles. Overall, this shows the effort of researchers for improving the magnetic adsorbent and the important of this work. However, Most of the magnetic adsorbent still require multi-step and complicated processes for increasing the surface area and porosity of materials. Moreover, they also used high temperature and toxic and expensive chemicals.

Therefore, in this study, a less complicated and more environmentally friendly will be used (Kharissova et al., 2015).

Liu and coworkers (2012) was successfully produced a very easy improvement of bio-char by alkali and acid as an adsorbent for a tetracycline (TC) adsorption. The resulting materials indicate that the alkali treated bio-char present the surface area higher than acid treated bio-char and also the raw material. Furthermore, this alkali treated bio-char also illustrates the excellent adsorption performance of tetracycline as high as 58.8 mg/g that higher than those acid treated bio-char and raw material. In addition, the graphite-like structure of alkali treated bio-char accommodates the formation of **π–π** interactions between TC structure and graphite-like sheets. The surface area represented important ascendants on the adsorption of TC and also O-containing functional groups, unless the initial pH of solution has minor ascendants on TC adsorption under the experimental conditions. Furthermore, more pores in bio-chars may 'trap' more TC molecules. Thus, the adsorption performance of this adsorbent on TC molecules can be succeeded by increasing the BET surface area and also the pore size distribution of adsorbent (Liu et al., 2012).

Zhang and coworkers (2019) was successfully explored the possibility of applying cow manure biochar (CMBC) for tetracycline adsorption for understanding farm waste remedy as well as recycling. From this study, there were several essential differences in the functional groups, specific surface area, pore structure and also surface charge. Thus, the ascendant in adsorption was not depended on the physicochemical properties of the adsorbent but also the room temperature, the dosage and solution pH. In addition, the interaction between the oxygen-containing functional groups on the surface of CMBCs and the hydroxyl group in the tetracycline is thought to occur by hydrogen bonds and **π-π** electron donor-acceptor interactions, accounting for the rapid adsorption of tetracycline (Zhang et al., 2019).

Mehta and coworkers (2015) reviewed The review article endeavors to diagnose and examine a spacious formation of magnetic adsorbents for the removal of various kind of pollutants for example organic pollutants, dyes heavy metals as well as non-metals in water solution. The employment of magnetic adsorbents proposes an important good point more than several adsorbents that is the potentiality to

differentiate them from a water solution on application of a magnetic property. From previous research studies illustrated that the mechanism of adsorption behavior such adsorption isotherm and adsorption kinetics depended on the adsorbent surface like chemical nature, the pore textures and also the experimental conditions for example temperature, contact time, initial pollutant concentration, pH and also adsorbent dosage and so on. Moreover, there were almost adsorbents followed both Freundlich adsorption isotherm and Langmuir adsorption isotherm. In addition, these 2 models could be applied to measure the ability of adsorption of various adsorbents. In addition, for the kinetics models, pseudo second order model was followed by the quantity of adsorbents. Although plenty of previous works considering magnetic adsorbents is obtainable besides it is accumulating at a spacious step everyday but there still remains various intervals that require to be addressed (Mehta et al., 2015).

So far as we know, there are no report on the preparation of magnetic carbon adsorbent from sugarcane bagasse and Fe^{2+} and Fe^{3+} via simultaneous magnetization and activation process. Hence, this research study represents novel materials and facile preparation to create magnetic porous carbon adsorbents by simultaneous magnetization and activation method for removal of tetracycline from aqueous solution.

1.4 Objectives

- To synthesize magnetic porous carbon materials derived from sugarcane bagasse and characterize these materials with various techniques.
- To methodically examine the effects of physical property such pore texture and pore size and also chemical property of the adsorbents towards tetracycline in terms of kinetics and isotherm.

CHAPTER 2

EXPERIMENTAL

2.1 Chemicals and materials

1. Ferrous sulfate heptahydrate ($FeSO_4.7H_2O$, 99.5%) was purchased from Sigma-Aldrich.
2. Ferric chloride hexahydrate ($FeCl_3.6H_2O$, 99.0%) was purchased from Loba Chemie.
3. NaOH (97.0%) and HCl (37%) were purchased from J.T. Baker.
4. Sugarcane bagasse (Saccharum officinarum L., composed of cellulose ~40–50%, hemicellulose ~25– 35%, lignin ~15–25% and minor amounts of mineral)[19] was obtained from Eastern Sugar and Cane Public Company Limited, Sa Kaeo province of Thailand, and was used as the carbon precursor.
5. Deionized (DI) water was used for all experiments, and all chemicals were AR grade.
6. Tetracycline ($C_{22}H_{24}N_2O_8 \cdot xH_2O$) was purchased from Sigma-Aldrich.
7. Syringe Filter Nyron 0.45 μm, 13 mm, CHROM FILTER.
8. Disposable Syringe 5 mL, NIPRO.

2.2 Equipment and instruments

1. N_2 sorption analysis (Micromeritic, ASAP 2460) at 77 K.
2. X-ray diffraction (XRD, Philips, X'Pert MPD, Netherlands) was employed to identify the iron phase.
3. X-ray photoelectron spectroscopy (XPS, AXIS Ultra DLD, Kratos Analytical Ltd.) was used to investigate both quali- and quantitatively C, O, and Fe species.
4. Vibrating Sample Magnetometry (VSM, Lakeshore) was carried out at 298 K
5. Field Emission Scanning Electron Microscopy with Energy Dispersive X-Ray Spectroscopy (FESEM-EDX, Quanta 400, FEI) were used to investigate the surface texture and their iron particle distribution.
6. Tube Furnace (Carbolite)

2.3 Methods

2.3.1 Preparation of magnetic porous carbon materials

Firstly, collected sugarcane bagasse after 3-cycle squeezing out of nectar was washed to remove leftover sugar, dirt and other impurities with deionized water (DI) several times. Then the samples were dried at 100 ℃ for 48 hours. The cleaned sugarcane bagasse was ground and sieved into 70-mesh particles (BG). In a typical synthesis, 15.00 g of BG was soaked at ambient temperature under stirring conditions with 120 mL of Fe^{2+}/Fe^{3+} solution with 1:2 Molar ratio for 1 hour. The predicted weight ratio of BG:Fe_3O_4 was 1: 0.125; hence, 2.25g $FeSO_4 \bullet 7H_2O$ and 4.38g $FeCl_3 \bullet 6H_2O$ were employed. Afterwards, 62 mL of DI water was mixed with 38 mL a NaOH solution. NaOH concentrations of 0.2, 0.5 and 1.0 M were selected to study its effect on the materials properties. Then, the clear base solution was added into the mixture of dried sugarcane bagasse and Fe^{2+}/Fe^{3+} solution. The resulting mixture was hence stirred at ambient temperature for 2 hours at a stirring rate of 3.5 Mot. Subsequently, the mixture of BG soaked with NaOH and Fe^{2+}/Fe^{3+} solutions for 24 hours at ambient temperature was followed by being heated in an oven at 80 °C for 3 days in order to evaporate the water. The reference material was prepared following a similar method without the addition of NaOH; furthermore, 100 mL of DI water can be used instead of NaOH solutions.

The dried samples were labeled as MBG(x) where MBG stands for magnetic carbon composite derived from sugarcane bagasse and x represents the concentration of NaOH in molar.

Optical images all of samples before pyrolysis are shown in Figures 11(a-d), (MBG(0), MBG(0.2), MBG(0.5) and MBG(1.0), respectively, where 0, 0.2, 0.5, 1.0 represent the concentrations of NaOH in M). These dried materials were then pyrolyzed at 800 °C under nitrogen atmosphere for 1 hour at a heating ramp of 5 °C/min. Then, the pyrolyzed samples were excessively washed with hot DI water until neutral pH was reached to dispose other inorganic contaminants. The magnetic carbon materials were named as MBG(x)-800 where 800 indicates the pyrolysis temperature.

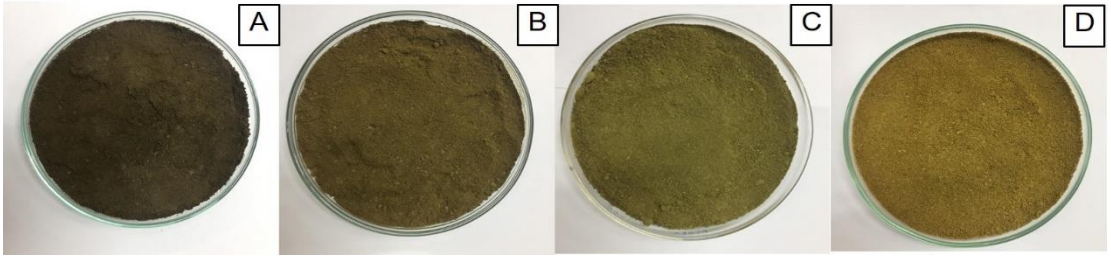

Figure 11. Optical images of (A) MBG(0), (B) MBG(0.2), (C) MBG(0.5) and (D) MBG(1.0) before carbonization process.

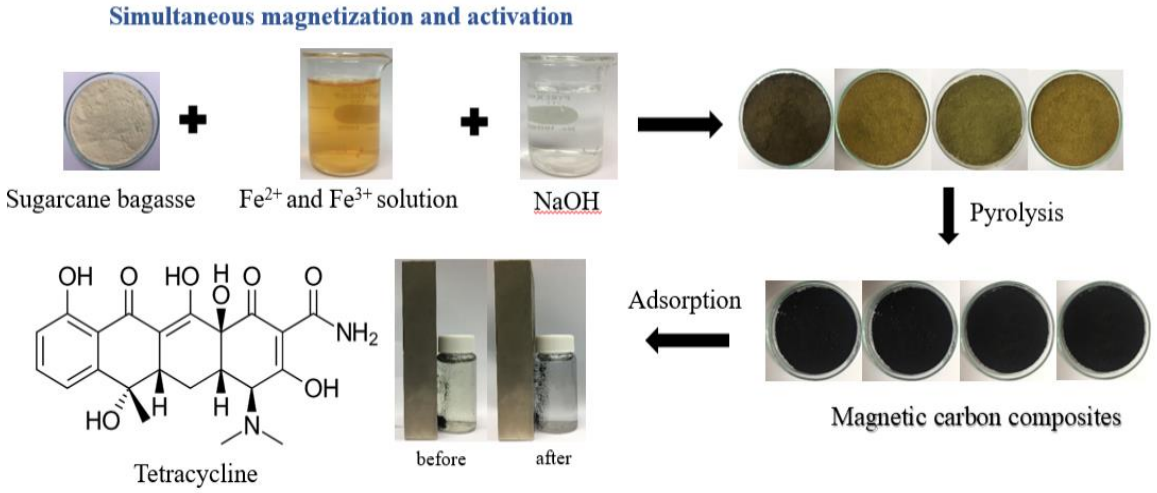

Figure 12. Schematic Illustration of the preparation steps for all samples.

2.3.2 Characterization of magnetic porous carbon materials

(1) Vibrating sample magnetometer (VSM) was applied to examine the magnetic moment which is the most fundamental quantity in magnetism of solid samples. To study the magnetic efficiency at 300 K, the signal is proportional to the vibration frequency, vibration amplitude and magnetic moment as well. The scan was run for applied magnetic field, H from -15,000 Oe to 15,000 Oe. Finally, this machine illustrates the magnetic moment in e.m.u.

(2) X-ray Powder Diffraction (XRD) was performed to identify the crystal structures and the forms of iron in the samples. The scan was run for 2*theta from 5° to 90°

(3) X-ray photoelectron spectroscopy (XPS) was used to determine the functional groups and the iron species on surfaces, both quantitatively and qualitatively.

(4) N_2 adsorption-desorption analysis was used for characterization in a high range of porous carbon composites. This technique can apply for the examination of new composites and quality control also. In addition, the examination of adsorption isotherms uses the temperature of liquid nitrogen at around 77 K. The specific surface area and pore size distribution examine by BET-nitrogen method and BJH methods, respectively (Sing, 2001).

(5) Scanning electron microscopy equipped with energy dispersive X-ray spectroscopy (SEM EDX) was used to study the surfaces and morphology of the magnetic particles.

2.3.3 Adsorption studies

2.3.3.1 Adsorption Kinetics and Adsorption isotherm

To study the adsorption efficiency of the adsorbent materials towards TC, adsorption isotherm experiments were performed with 0.04 g of adsorbent and 20 mL of various TC concentrations. The mixture was then shaken for 4 days (96 hours) on a shaker incubator (Model TOL09-FTSH-01, SCIFINETECH) at ambient temperature (30±2 ^{o}C) to reach equilibrium.

To investigate the adsorption kinetics for the adsorption of TC, the adsorption kinetics was operated similarly to adsorption isotherm using 100 ppm of TC solution in different time intervals (0–96 hours) in a neutral pH (6.8). In each isotherm and kinetic experiment, after complete adsorption, the magnetic carbon adsorbent was easily separated from the solution using an external magnet. The concentrations of TC before and after adsorption were determined using a calibration method, with UV–Vis spectrophotometer (UV 2600, Shimadzu) at λ = 357 nm.

CHAPTER 3

RESULTS AND DISCUSSION

3.1 Optical images of resulting samples before carbonization process

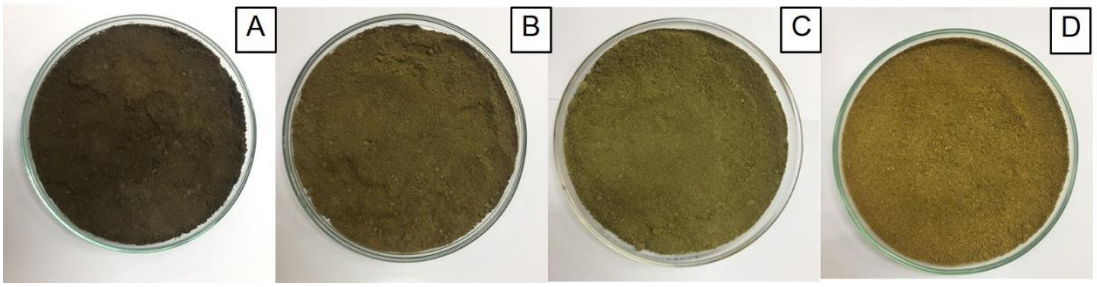

Figure 13. Optical images of (A) MBG(0), (B) MBG(0.2), (C) MBG(0.5) and (D) MBG(1.0) before carbonization process

Optical images of resulting samples show the difference color depend on NaOH adding in samples.

3.2 Characterization of magnetic porous structures

The preparation process proposed in this study can be considered expedient and proper for large-scale synthesis of magnetic carbon adsorbent material *via* simultaneous magnetization and activation process in a single step. The XRD patterns for as-prepared sample (MBG(1.0)) and all of pyrolyzed samples (MBG(0)-800, MBG(0.2)-800, MBG(0.5)-800 and MBG(1.0)-800)) are illustrated in Figure 14(A-B). MBG(1.0) sample illustrates a relatively broad typical pattern of XRD, which proves that the as-prepared sample possessed no crystalline iron particles (Figure 14A). On the contrary, the XRD patterns of MBG(0)-800, MBG(0.2)-800, MBG(0.5)-800 and MBG(1.0)-800 all demonstrate the similar characteristic diffractions of crystalline magnetite particles (Fe_3O_4) with diffraction peaks at 2θ = 18.3°, 30.1°, 35.5°, 37.1°, 43.1°, 53.5°, 57.0°, 62.6° and 74.1° as presented in Figure 14 the existence of Fe_3O_4 particles from XRD patterns confirms a successful conversion of non-magnetic iron

ions (Fe^{2+} and Fe^{3+} ions) into the iron magnetite (Fe_3O_4) phase by uncomplicated precipitation coupled with a subsequent pyrolysis

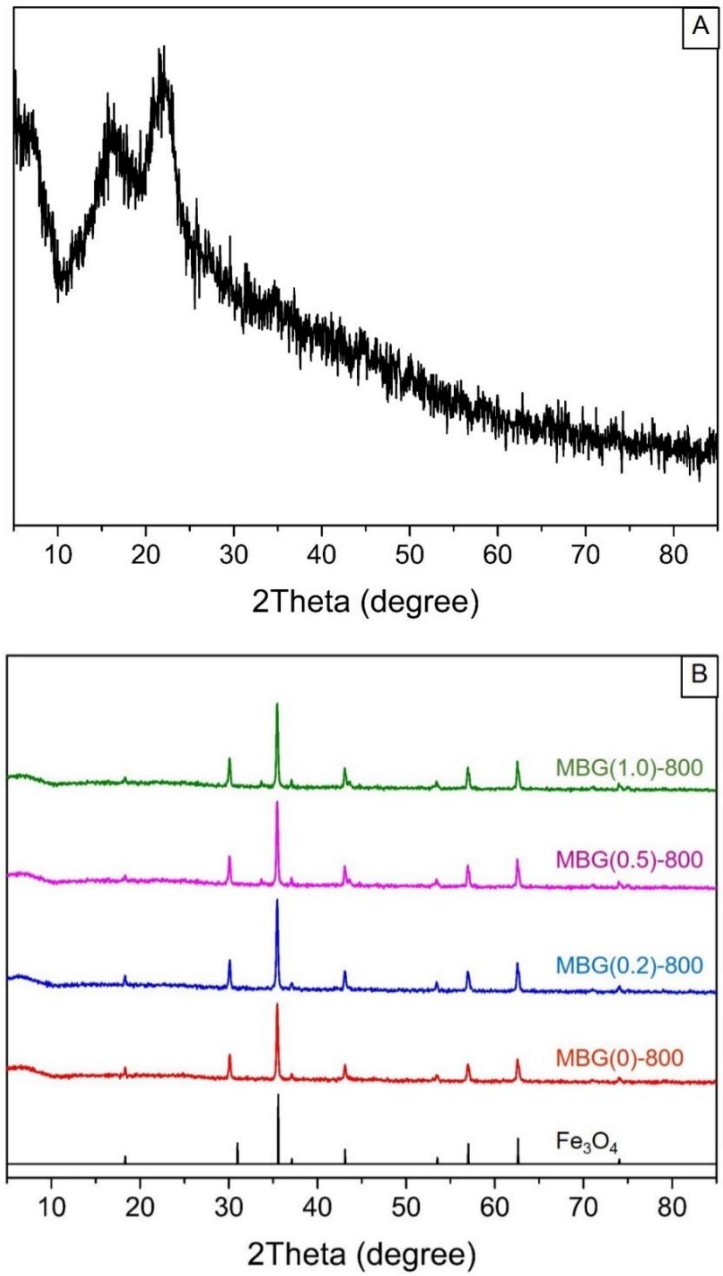

Figure 14. XRD patterns of (A) as prepared sample MBG(1.0) and (B) MBG(0)-800, MBG(0.2)-800, MBG(0.5)-800 and MBG(1.0)-800.

To verify the development of porosity of the resulting materials and to study the effect of NaOH on the porosity, N_2 sorption analysis was carried out. The N_2 sorption isotherms of MBG(0)-800, MBG(0.2)-800, MBG(0.5)-800 and MBG(1.0)-800 apparently belong to the type IV isotherm (IUPAC classification), as shown in Figures 15(A-D). The isotherms of MBG(0)-800 and MBG(0.2)-800 demonstrated a small hysteresis loop; furthermore, MBG(0.5)-800 and MBG(1.0)-800 illustrated a larger hysteresis loop. By calculating using t-plot method, the isotherms of MBG(0)-800, MBG(0.2)-800, MBG(0.5)-800 and MBG(1.0)-800 are reflective of a large amount of mesopores (61.74, 63.12, 64.08 and 81.50 v% respectively) and smaller fractions of micropores (38.26, 36.88, 35.92 and 18.50 v%, respectively). The samples MBG(0)-800, MBG(0.2)-800, MBG(0.5)-800 and MBG(1.0)-800 contained BET surface areas of as high as 429, 433, 663 and 566 m^2/g and total pore volumes of as high as 0.21, 0.21, 0.39 and 0.33 cm^3/g, respectively. Porous textural properties measured by nitrogen sorption of all carbon composites are shown in Table 1. Obviously, the simultaneous activation and magnetization process purposed in this work can lead to the formation of mesoporosity along with *in situ* formation of magnetite particles in the samples without further impregnation of magnetic particles after activation. The purposed method can reduce the time consumption for the whole preparation, which can suitably be applied to the large scale production. Moreover, the presence of large fraction of mesoporosity is useful in adsorption of large toxic molecules, like TC in this case.

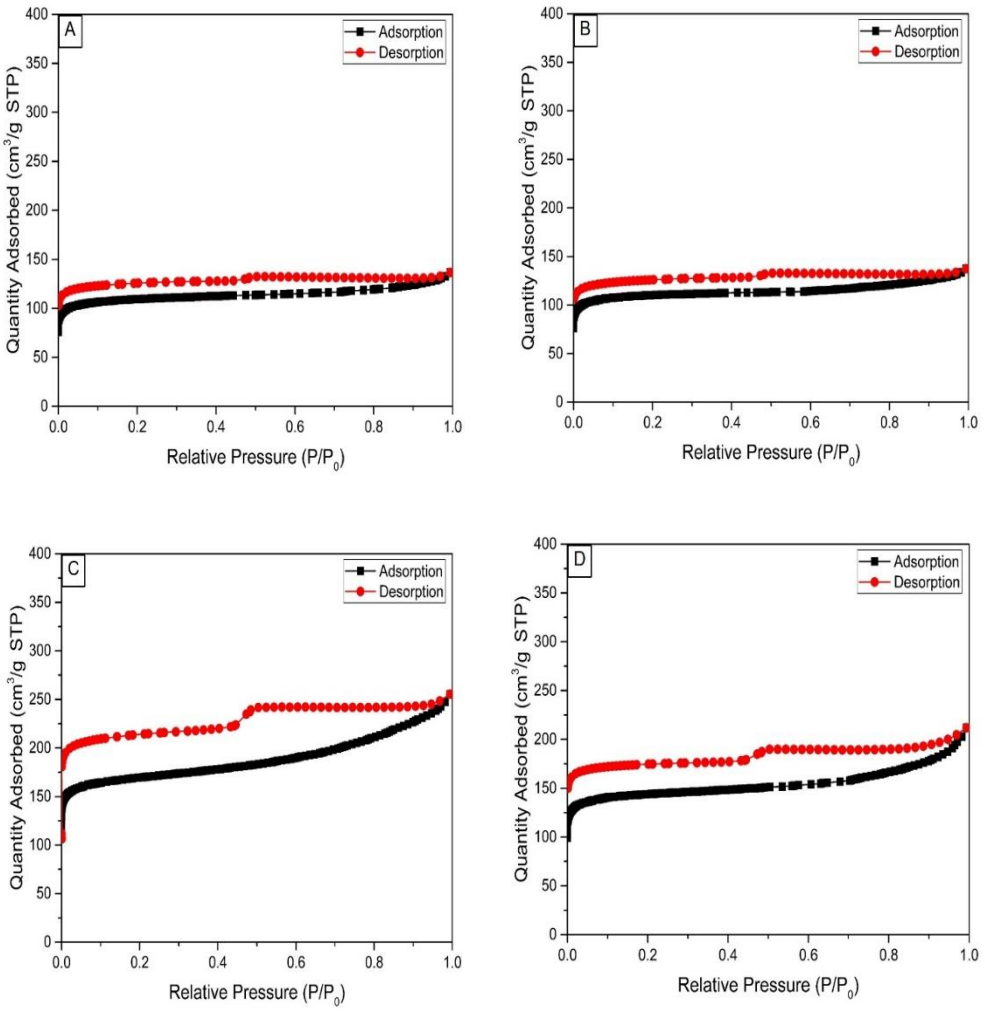

Figure 15. Nitrogen adsorption-desorption isotherms of (A) MBG(0)-800, (B) MBG(0.2)-800, (C) MBG(0.5)-800 and (D) MBG(1.0)-800.

Table 1. Porous textural properties measured by nitrogen sorption at 77K.

Samples	Surface area (m^2/g)			Pore Volume (cm^3/g)			%
	BET	Micro[a]	Meso[b]	Total[c]	Micro[d]	Meso[e]	Meso pore
MBG(0)-800	429.44	173.84	255.60	0.211	0.081	0.130	61.74
MBG(0.2)-800	433.12	164.59	268.53	0.212	0.078	0.134	63.12
MBG(0.5)-800	663.85	321.50	312.35	0.394	0.142	0.253	64.08
MBG(1.0)-800	566.07	44.82	521.25	0.328	0.061	0.267	81.50

[a] t-plot micropore area

[b] t-plot external surface area

[c] total pore volume

[d] t-plot micropore volume

[e] difference of total pore volume and micropore volume

[f] BJH adsorption average pore diameter

[g] DFT pore size

Although all the prepared magnetic composites contribute large amounts of mesopores, more detailed analysis on the pore size distribution of the samples can be used to investigate the effect of addition of different NaOH on the pore characteristics. In spite of the largest BET surface area of MBG(0.5)-800, it contains smaller mesopore volume and area in comparison with those of MBG(1.0)-800. The pore size distributions plotted *via* both DFT and BJH models (Figures 16 and 17, respectively) obviously show the larger contribution of the mesopore size in the range of 2-10 nm for MBG(0.5)-800 and MBG(1.0)-800 than for MBG(0)-800 and MBG(0.2)-800. According to the N_2 sorption results, it is expected that the more NaOH was used, the more mesoporosity can be generated. This similar behavior has also been observed in the previous works (Martins et al., 2015). While the magnetite particles can similarly be obtained in all materials prepared with NaOH, the posority of the BG-based magnetic porous carbons can be fine-tuned by controlling NaOH amount.

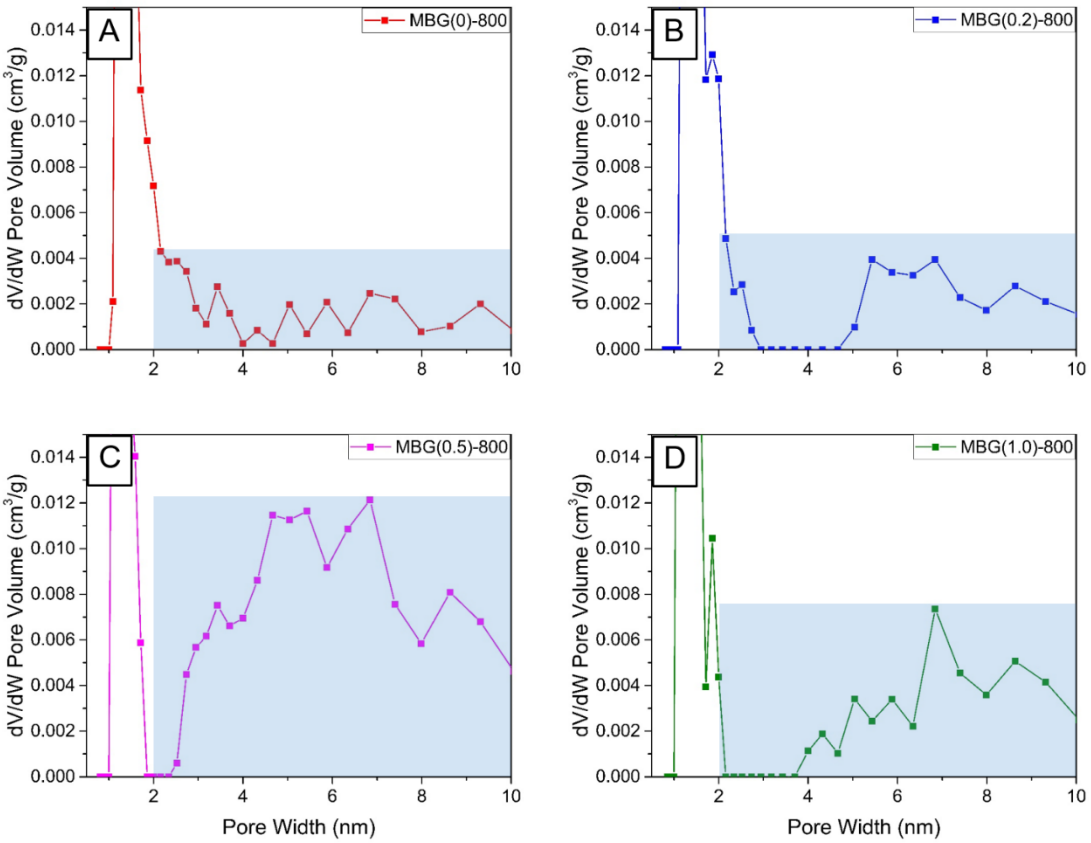

Figure 16. Pore size distributions using DFT model of (A) MBG(0)-800, (B) MBG(0.2)-800, (C) MBG(0.5)-800 and (D) MBG(1.0)-800.

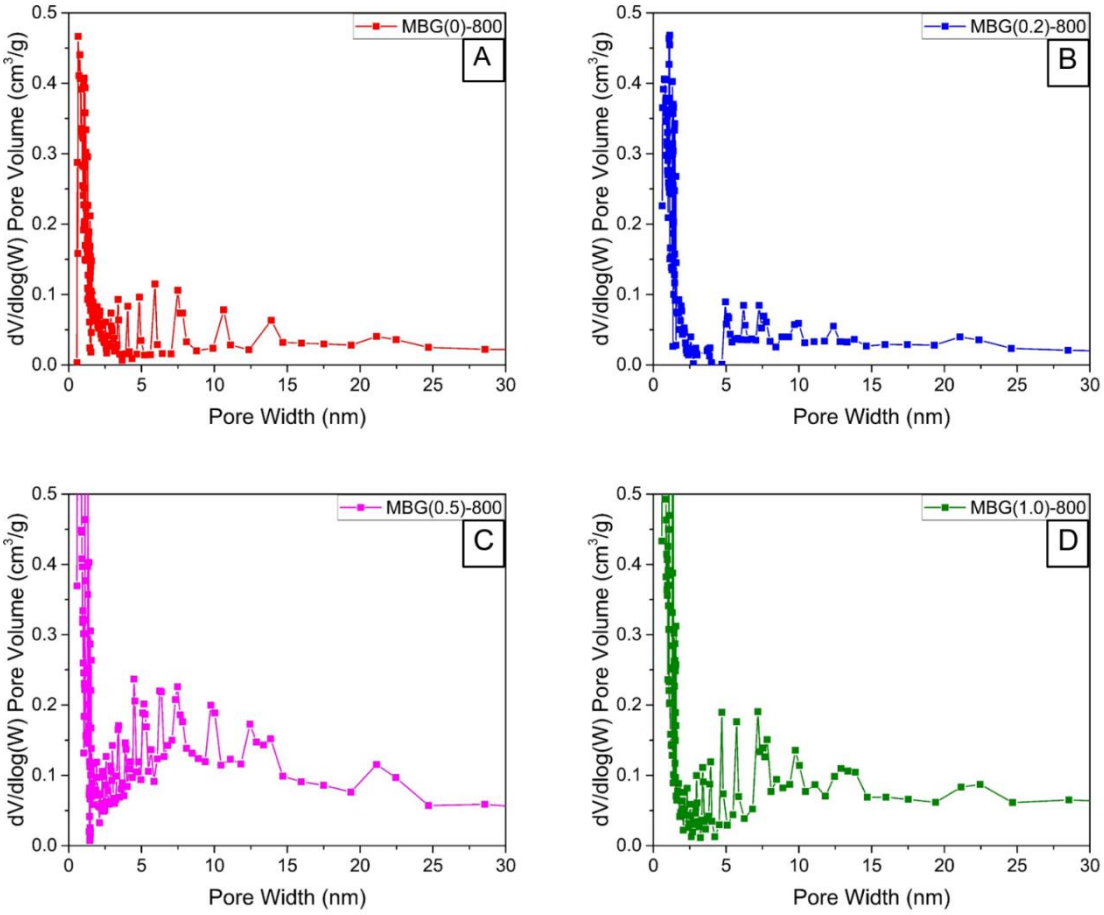

Figure 17. Pore size distributions using BJH model of (A) MBG(0)-800, (B) MBG(0.2)-800, (C) MBG(0.5)-800 and (D) MBG(1.0)-800.

The elemental composition and bonding relationship for all of adsorbent materials were analyzed by XPS, as shown in Figure 18 and Figure 19(A-L). Survey scan in Figure 18 illustrates that the elemental composition of all samples was composed of C 1s, O 1s and Fe 2p, appearing at binding energies of 284.5, 532.0 and 710.38 eV, respectively. Because of the low concentration of iron in the system, the Fe 2p peak intensities for all adsorbent samples were relatively low. XPS analysis illustrating the C, O and Fe contents are shown in Table 2, indicating that all obtained samples show the high carbon contents over than 70 % by weight. C 1s and O 1s high resolution spectra of all samples are demonstrated in Figure 19(A-H). The bonding relationship of all samples is demonstrated at binding energies ~284, ~286, ~287, ~288 and ~289 eV corresponding to C=C, C-O, C=O, O-C=O and COOH, respectively. sp^2 carbon shows the highest intensity which is a typical behavior of the pyrolyzed carbons from biomass at the temperatures over than 700°C. Furthermore, O 1s high resolution of all samples displayed the bonding between Fe-O at ~532 eV, associating with XRD result of Fe_3O_4.

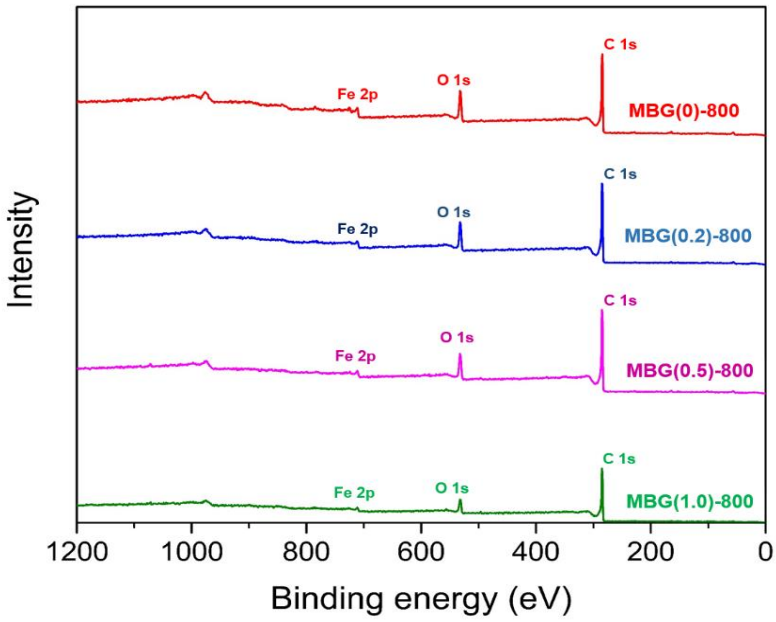

Figure 18. XPS survey spectra of MBG(0)-800, MBG(0.2)-800, MBG(0.5)-800 and MBG(1.0)-800.

Table 2. The percentage compositions from XPS analysis of all samples.

Samples	%C		%O		%Fe	
	by atomic	by weight	by atomic	by weight	by atomic	by weight
MBG(0)-800	83.24	72.55	13.87	15.88	2.89	11.57
MBG(0.2)-800	85.87	77.55	12.24	14.59	1.89	7.86
MBG(0.5)-800	86.51	79.63	12.08	14.47	1.41	5.90
MBG(1.0)-800	88.82	83.02	10.14	12.49	1.04	4.49

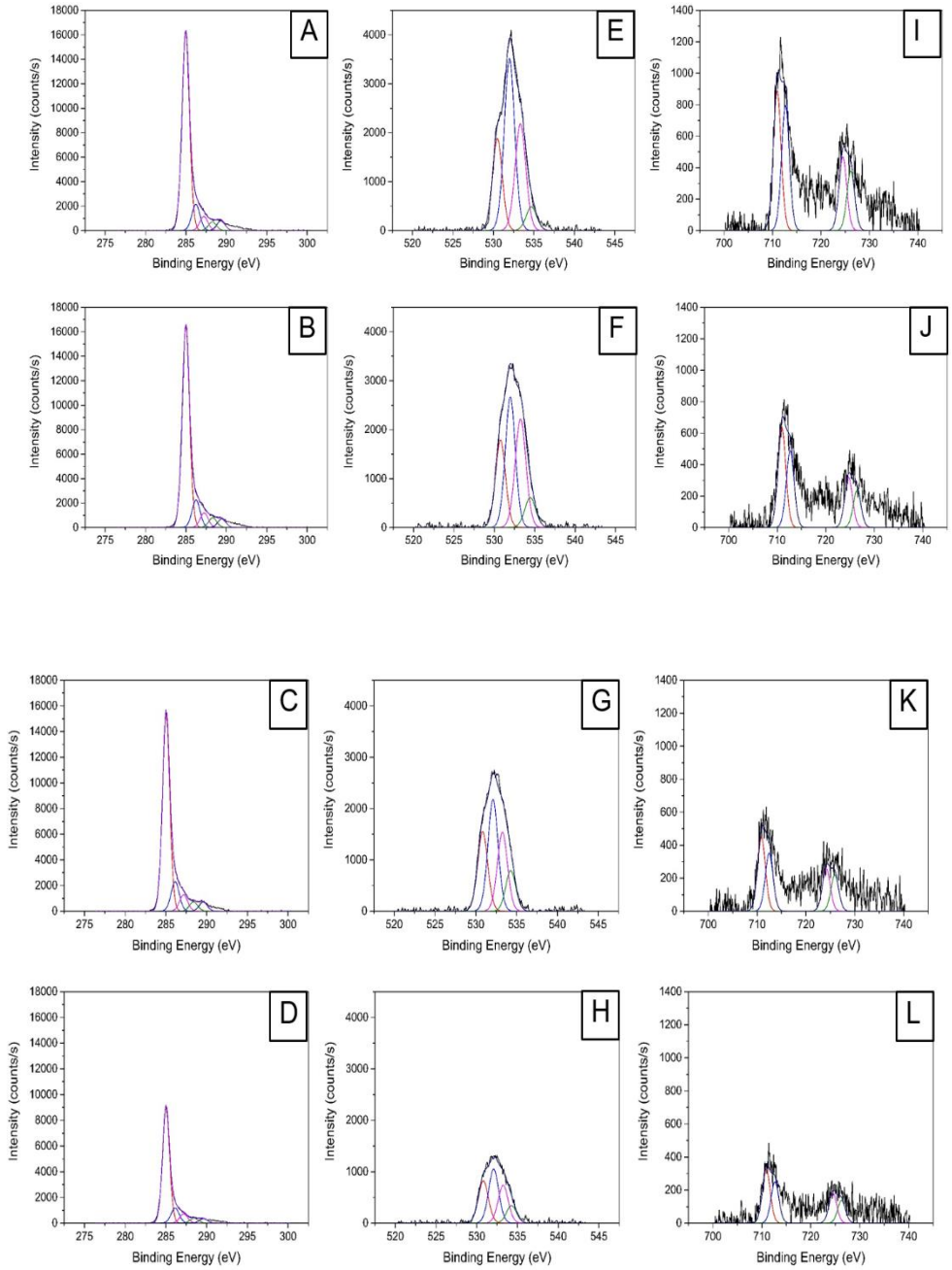

Figure 19. XPS profiles representing (A-D) C 1s, (E-H) O 1s and (I-L) Fe 2p high-resolution spectra of MBG(0)-800, MBG(0.2)-800, MBG(0.5)-800 and MBG(1.0)-800 (L) of MBG(1.0)-800 (the series of all sample sets is in a vertical order, respectively).

The high carbon content from the XPS information indicates the possession of marked C in the form of dominant sp^2 structure, which is a typical character of the pyrolyzed carbons from biomass. The presence of dominant sp^2 carbon could therefore be used to explain the adsorption interactions between the sample surface and TC molecules in the aqueous system.

Even though the Fe content in the feature of Fe_3O_4 for the entire samples was not massive, the magnetic properties of MBG(1.0)-800 is acceptable. The very good magnetic behaviors of the resulting magnetic carbon adsorbent are shown in Figure 20(A-B). The hysteresis loop estimated from VSM measurement of MBG(1.0)-800 is indicated in Figure 20(A). The VSM curve illustrates a very huge hysteresis with symmetric magnetization curves, suggesting a great superparamagnetic qualification, which is consistent with the presence of Fe_3O_4 in the XRD results. MBG(1.0)-800 sample presents the saturation magnetization value of 20.72 emu/g, confirming sufficient magnetization for potential application in sample separation from water solution. The excellent magnetic capability and stability of MBG(1.0)-800 is further confirmed using the photographs of magnetic separation of the adsorbent in Figure 20(B), even after complete TC adsorption for 24 hour. Outstandingly, MBG(1.0)-800 was readily separated from water by an external magnet, and the entire sample particles could exhaustively be attracted within only 3 minutes.

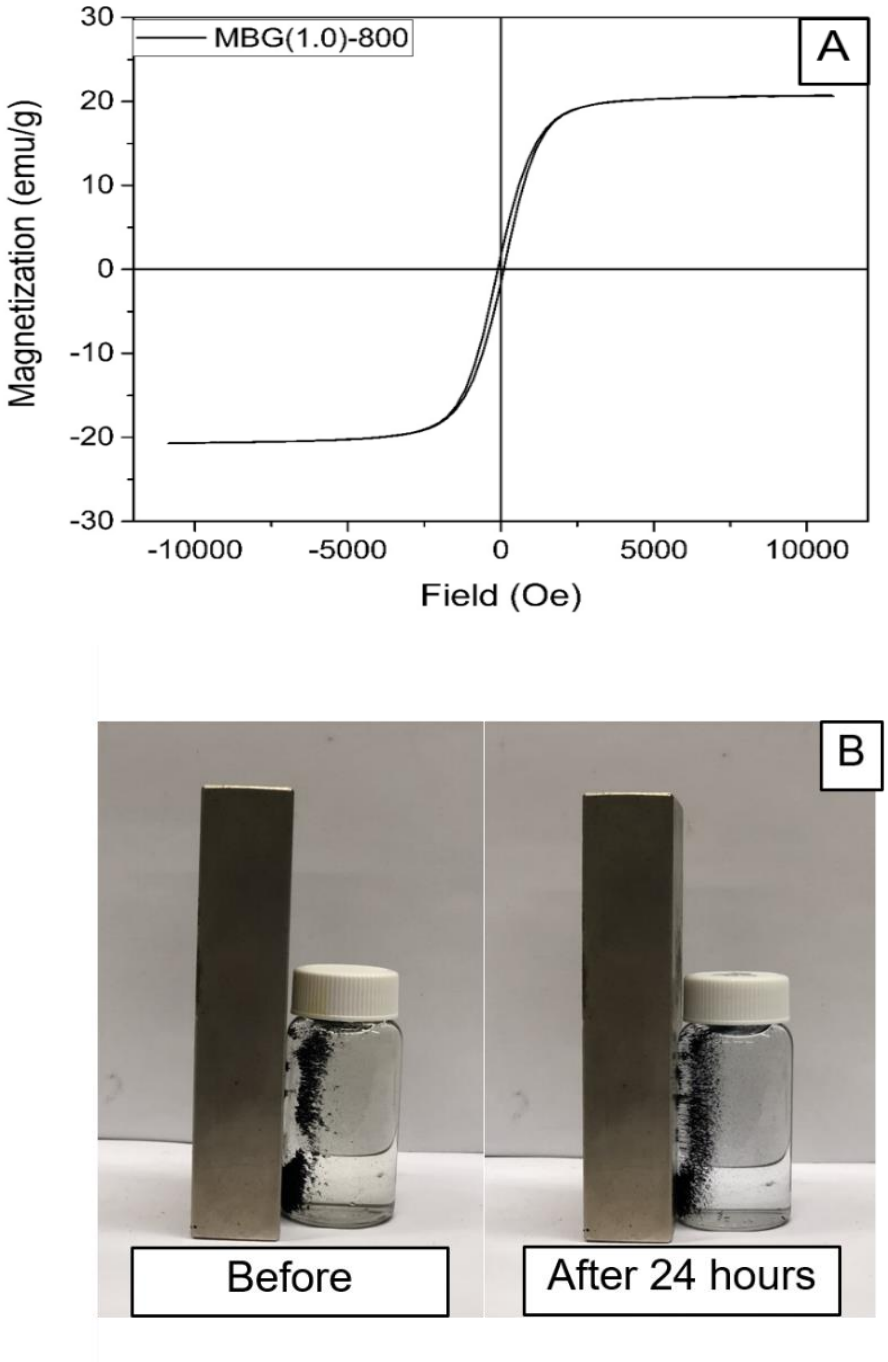

Figure 20. (A) Magnetization curve of MBG(1.0)-800 obtained by vibrating sample magnetometer (VSM) at room temperature and (B) the magnetic properties before and after the adsorption towards TC (20 mg/L, 20 mL) of the sample.

3.3 Adsorption of TC by magnetic porous carbon materials

3.3.1 Adsorption isotherm and adsorption kinetics toward TC by magnetic porous carbon materials

The adsorption performance towards TC on MBG(0)-800, MBG(0.2)-800, MBG(0.5)-800 and MBG(1.0)-800 was studied. The outcomes of adsorption isotherm in Figure 21 illustrated that the maximum adsorption capacity of TC on MBG(0)-800, MBG(0.2)-800, MBG(0.5)-800 and MBG(1.0)-800 are 19.00, 24.15, 38.25 and 48.40 mg/g, respectively. The determination coefficient (R^2) of the non-linear Langmuir model equals to 0.9994 for MBG(1.0)-800. Also this sample shows the highest capacity adsorption. This indicates that the isothermal information was appropriated explained with the Langmuir model, suggesting the monolayer formation.

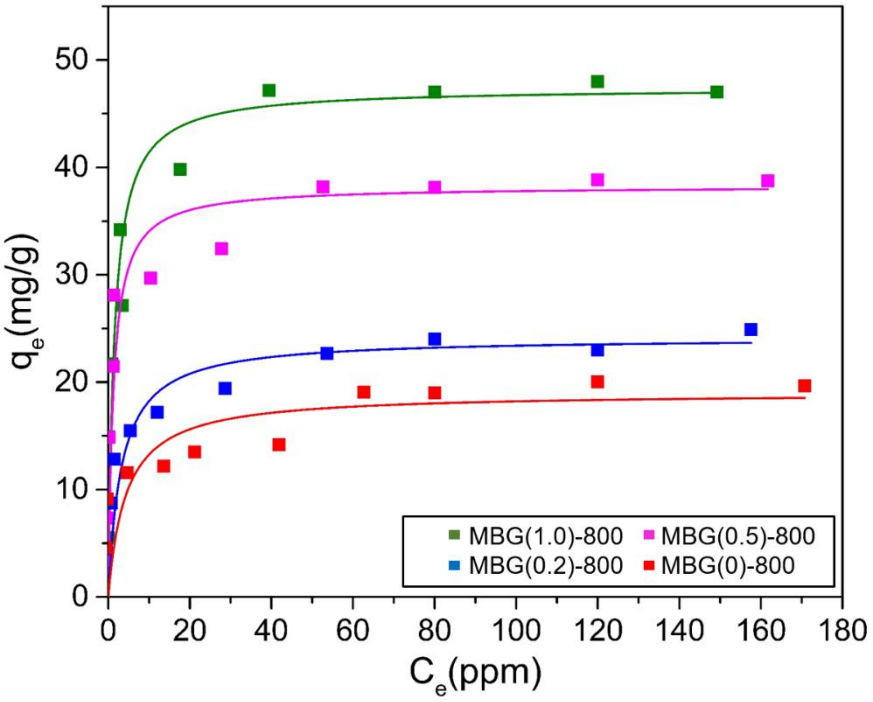

Figure 21. Adsorption isotherms of TC onto all samples. Reaction conditions: initial concentrations of 10-200 ppm, temperature 30±2 °C and adsorbent dosage of 0.04 g with 20 mL of TC solutions.

Since MBG(1.0)-800 showed the highest adsorption among all, the sample was then selected for studying the adsorption kinetics, and the result is shown in Figures 22. The adsorption amount of TC onto MBG(1.0)-800 increased gradually in the first 50 hours and reached adsorption equilibrium around 60 hours, presenting a slow adsorption kinetic. The adsorption kinetics was appropriately fitted with pseudo-second-order model for TC adsorption, with the determination coefficients (R^2) of 0.9999. The adsorption performance of the adsorbent displayed in this work is relatively identical to or even higher than that of several adsorbents reported in literatures shown in Table 3.

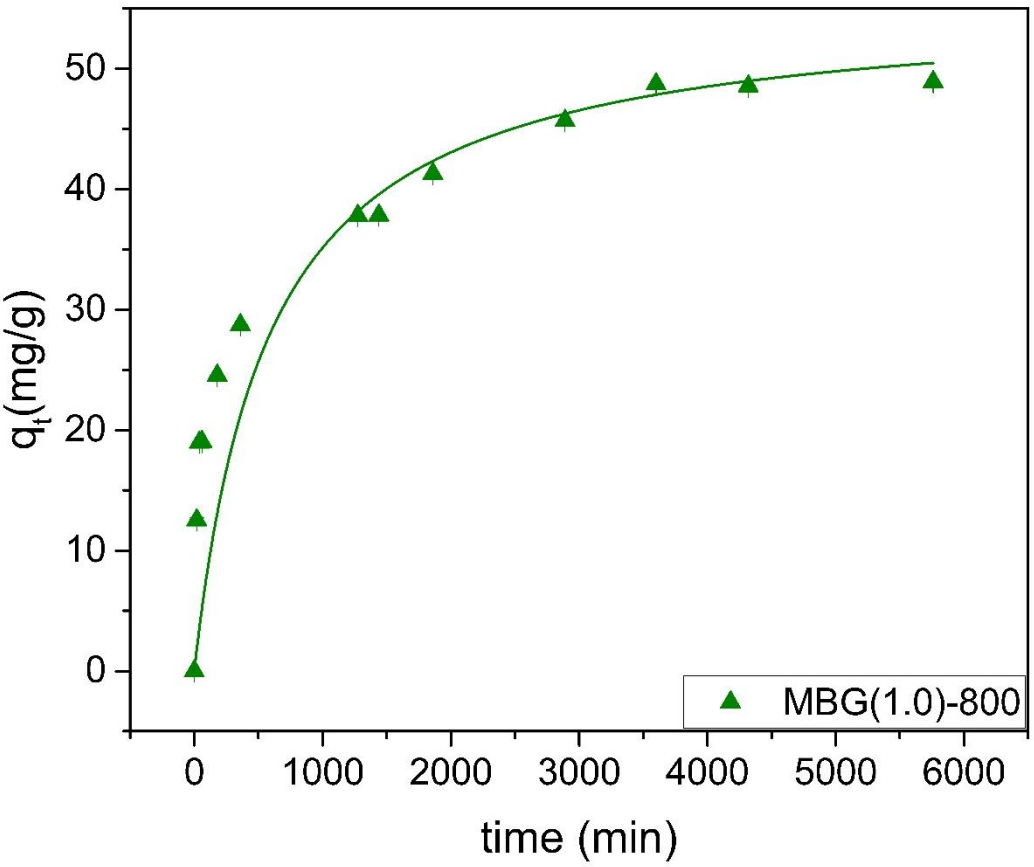

Figure 22. Adsorption kinetics of TC onto MBG(1.0)-800. Reaction conditions: initial concentration of 100 ppm, temperature 30±2 °C and adsorbent dosage 0.04 g with 20 mL of TC solution.

Table 3. Comparison with literature data on material adsorbents for TC removal and results from the current studies.

Materials/Adsorbent	Precursor	Method	S_{BET} (m^2/g)	q_m (mg/g)	Ref
Graphene oxide functionalized magnetic particles (GO-MPs)	Graphene oxide	Amine-functionalization method	-	39.1	(Lin et al., 2013a)
Magnetic porous carbon with maghemite particles (MPC)	Waste hydrochar	Simultaneous activation and magnetization method	349	25.44	(Zhu et al., 2013)
Rice husk ash (RHA)	Agricultural waste	-	-	8.37	(Chen et al., 2016)
Raw Bio-char	Bio-char	-	34.4	16.95	(Liu et al., 2012)
Alkaline Bio-char	Bio-char	Alkali treated	117.8	58.82	(Liu et al., 2012)
Acid Bio-char	Bio-char	Acid treated	46.8	23.26	(Liu et al., 2012)
Chitosan	Chitosan	-	-	13.3	(Kang et al., 2010)
Magnetic carbon composite (MBG(1.0)-800)	Sugarcane bagasse	Simultaneous activation and magnetization method	566	48.40	**This work**

The morphology and the chemical composition on the adsorbent composites were examined interlacing in the formation of Fe_3O_4, the characterization technique was employed and shown in detail below. The characterization of the adsorbent morphology was performed using SEM-EDX technique for MBG(1.0)-800, the best candidate adsorbent (**Figure 23).** The presence of C O and iron particles appears to be homogeneously distributed according to the EDX mapping shown in **Figure 23(C-E).** The average iron content was 4.1 wt%. This observation is consistent with the presence of iron determined by the XRD results in **Figure 14**, which indicates that MBG(1.0)-800 contained magnetite (Fe_3O_4) particles.

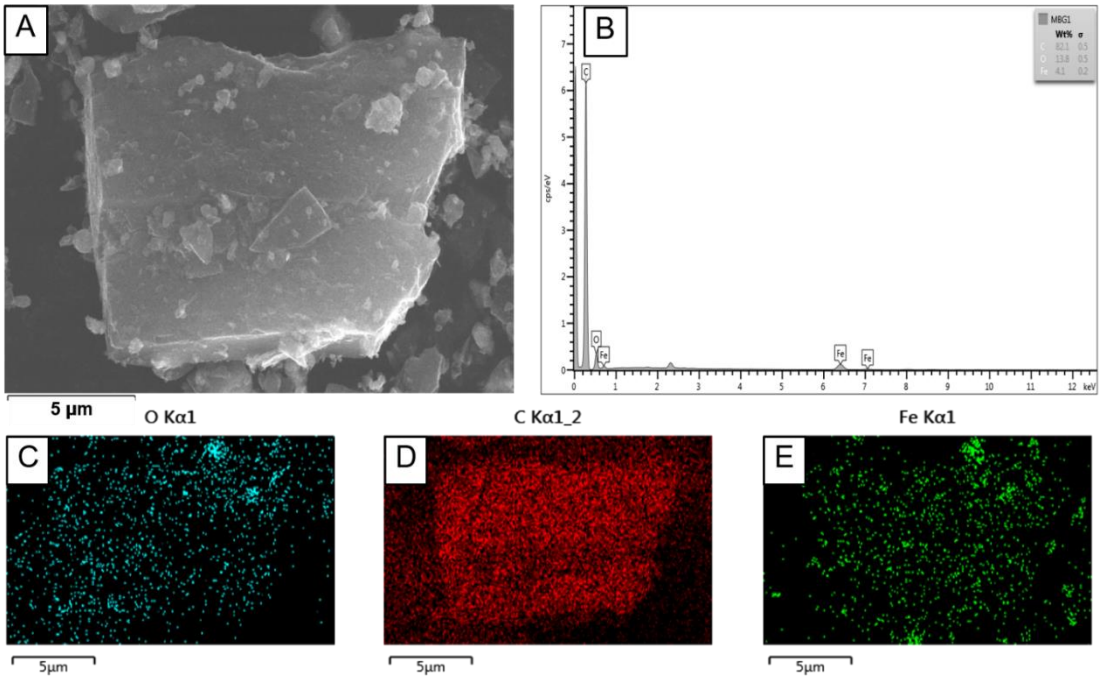

Figure 23. SEM-EDX analysis for MBG(1.0)-800. (A) SEM image at 20000× (B) EDX spectra and (C-E) EDX elemental mapping for O, C and Fe elements.

The examination of adsorption mechanism by employing the results from materials characterization is quite essential for ones to understand and to be able to tune surface chemistry and texture of the adsorbent for the future work. In general, the adsorption mechanism is affected by various parameters such as surface chemistry

and pore structure. Accordingly, the impact of these parameters on both adsorption performance and mechanism has to be concerned. In accordance with N_2 adsorption-desorption, XRD and XPS results discussed above, XPS essentially proved that the surface of all the magnetic composites prepared in this work possessed similar contents of C=C sp^2 carbon with similarity in oxygen amount and functionality. This implies that all adsorbents should possess the identical surface chemistry. Thus, all prepared adsorbents were dominated by the sp^2 character rather than the oxygen functionality. Therefore, π-π interaction could be reasonably used to explain the adsorption interactions between the surface of the samples and TC molecules due to the presence of π-electron system on sample surface and the aromatic ring of TC molecule. This behavior has similarly been observed in the previous literatures, in which the carbon carbonized more than 700 $^{\circ}$C and the π-π interactions of the carbon surface and TC molecules were reported (Martins et al., 2015). This is also consistent with our own observation by measuring the surface charge of all samples. The surface charge for all samples was observed to be neutral (pH of the surface was about 6.8 by pH_{pzc} measurements), while the TC molecules are typically in the neutral form. Therefore, the electrostatic interactions can be ignored.

Regardless of identical surface-TC molecule interactions, the different adsorption performances are thus controlled by pore structure of the carbon composites. Intuitively, among all samples, one can expect that the sample with the highest S_{BET} surface area should give the largest adsorption capacity. However, it is not true in our case reported here. Although MBG(0.5)-800 possessed a S_{BET} surface area as high as 663 m^2/g, q_m values for TC adsorption was 38.25 mg/g, less than that by MBG(1.0)-800 with lower S_{BET} (q_m = 48.40 mg/g). Moreover, the poor correlations between TC adsorption capacity with the S_{BET} surface area, as well as the micropore volume and micropore area are apparently indicated in Figures 24(A-C). Because the TC molecule is considered a large, high MW molecule with the largest dimension about 1.40 nm, the TC molecules cannot access the micropores with the size smaller than 2 nm. Thus, the pore restriction by microporosity occurs for the TC molecules. Interestingly, in a sharp contrast, the relationships between TC adsorption capacity with mesopore area and mesopore volume are linearly noticeable as evidenced in

Figures 24(D-E), emphasizing the importance of mesoporosity for the adsorption of TC. The adsorption mechanism related to the impact of pore texture is proposed in Figures 25. MBG(0)-800 and MBG(0.2)-800 contain larger fraction of small micropores which TC molecules cannot enter, while MBG(0.5)-800 MBG(1.0)-800 show higher fractions of mesoporosity, especially the highest content of mesoporosity in MBG(1.0)-800. The later two then can render the easier accessibility of the TC molecules into the inside carbon adsorbents (Figure 25). This was also similarly reported by the previous works (Liang et al., 2008, Marzbali and Esmaieli, 2017, Li et al., 2017).

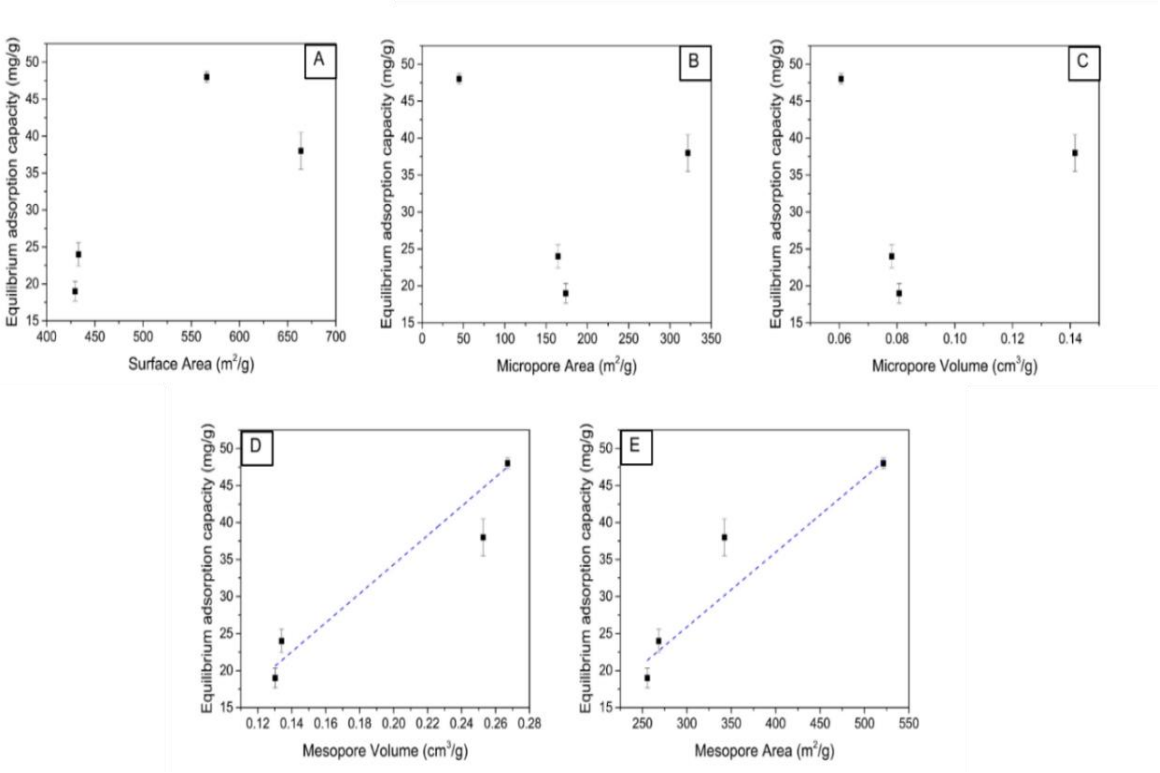

Figure 24. Correlation of adsorption affinity towards TC and different parameters (A) BET surface area (B) micropore area (C) micropore volume (D) mesopore volume and (E) mesopore area.

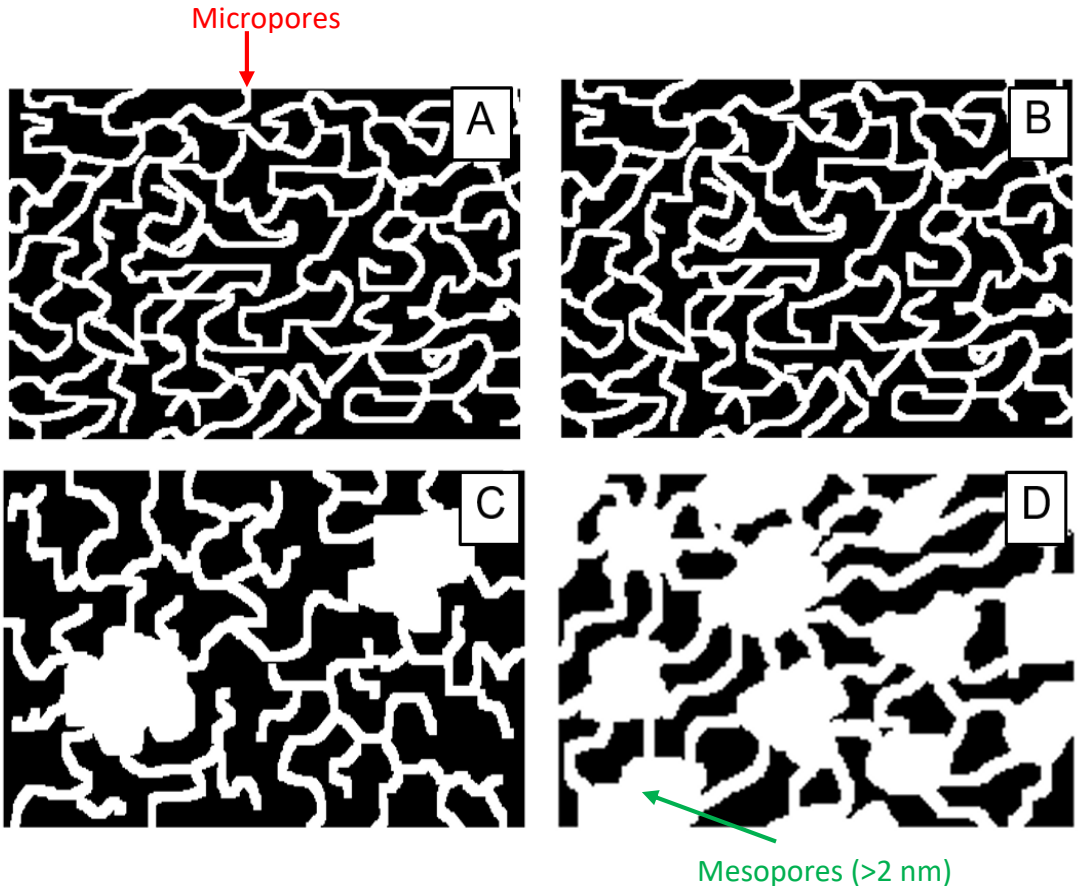

Figure 25. Representative illustrations of pore texture in different samples, (A) MBG(0)-800, (B) MBG(0.2)-800, (C) MBG(0.5)-800 and (D) MBG(1.0)-800.

In this work, we have shown that the large mesopore fraction can eventually be attained by a simple synthesis pathway. As proved by this work, sugarcane bagasse shows high potential as a carbon precursor for fabrication of mesoporous magnetic carbon composites. Moreover, the mesopores with diameters larger than 2 nm are regarded as "effective" pores for adsorption of the large antibiotic TC molecules.

To evaluate adsorption capability towards TC for MBG(1.0)-800, Table 3 summarizes and shows a comparison of q_m values with those from selected adsorbents. It is worth noting that a rather high TC adsorption capacity of MBG(1.0)-800 is comparable to those adsorbed by other adsorbents and also even predominates multifarious adsorbents from literatures. Besides its gently higher adsorption capabilities, preparation processes of the magnetic adsorbents should

also be taken into account. The preparation of adsorbents mostly requires multi-step processes and large quantity of toxic chemicals, resulting in higher costs of production and then making the scalability difficult. On the contrary, the preparation of the mesoporous magnetic carbon adsorbents reported in this work employed natural waste, sugarcane bagasse, as a carbon precursor. Our facile preparation strategy reported here not only lowers consumption of toxic chemicals, but also reduces costs and time of production, which is overall considered to be sustainable.

Considering the above facile synthesis purposed in this study, the wasted sugarcane bagasse can successfully be converted into mesoporous magnetic carbon adsorbents, which certainly helps shorten the time consumption in the industrial production. Furthermore, the use of abundant waste sugarcane bagasse as a carbon precursor could increase the country's income in a sustainable way.

CHAPTER 4

CONCLUSION

Mesoporous magnetic carbon adsorbents were successfully prepared using Fe^{2+} and Fe^{3+} ions as a magnetic precursor and sugarcane bagasse as a carbon source via a facile, one-pot synthesis and simultaneous magnetization/activation process. The adsorbent material can be used to adsorb TC from aqueous solution, representing the most adsorption capacity 48.40 mg/g for MBG(1.0)-800 sample with very large saturation magnetization value (20.72 emu/g). The concept of facile preparation reported here could lead to production of magnetic carbon-based adsorbents from other types of biomass.

BIBLIOGRAPHY

ÁLVAREZ-TORRELLAS, S., RODRíGUEZ, A., OVEJERO, G. & GARCíA, J. 2016. Comparative adsorption performance of ibuprofen and tetracycline from aqueous solution by carbonaceous materials. *Chemical Engineering Journal,* 283**,** 936-947.

BASTAMI, T. R. & ENTEZARI, M. H. 2012. Activated carbon from carrot dross combined with magnetite nanoparticles for the efficient removal of p-nitrophenol from aqueous solution. *Chemical Engineering Journal,* 210**,** 510-519.

BRAGHIROLI, F. L., BOUAFIF, H. & KOUBAA, A. 2019. Enhanced SO2 adsorption and desorption on chemically and physically activated biochar made from wood residues. *Industrial Crops and Products,* 138**,** 111456.

CAZETTA, A. L., PEZOTI, O., BEDIN, K. C., SILVA, T. L., PAESANO JUNIOR, A., ASEFA, T. & ALMEIDA, V. C. 2016. Magnetic Activated Carbon Derived from Biomass Waste by Concurrent Synthesis: Efficient Adsorbent for Toxic Dyes. *ACS Sustainable Chemistry & Engineering,* 4**,** 1058-1068.

CHANG, P.-H., LI, Z., JEAN, J.-S., JIANG, W.-T., WANG, C.-J. & LIN, K.-H. 2012. Adsorption of tetracycline on 2:1 layered non-swelling clay mineral illite. *Applied Clay Science,* 67-68**,** 158-163.

CHEN, Y., WANG, F., DUAN, L., YANG, H. & GAO, J. 2016. Tetracycline adsorption onto rice husk ash, an agricultural waste: Its kinetic and thermodynamic studies. *Journal of Molecular Liquids,* 222**,** 487-494.

DONG, H., JIANG, Z., ZHANG, C., DENG, J., HOU, K., CHENG, Y., ZHANG, L. & ZENG, G. 2018. Removal of tetracycline by Fe/Ni bimetallic nanoparticles in aqueous solution. *Journal of Colloid and Interface Science,* 513**,** 117-125.

DWIVEDI, K., MORONE, A., CHAKRABARTI, T. & PANDEY, R. A. 2018. Evaluation and optimization of Fenton pretreatment integrated with granulated activated carbon (GAC) filtration for carbamazepine removal from complex wastewater of pharmaceutical industry. *Journal of Environmental Chemical Engineering,* 6**,** 3681-3689.

E. DIEBEL, C., PROKSCH, R., GREEN, C., NIELSON, P. & M. WALKER, M. 2000. *Magnetite defines a magnetoreceptor*.

FOO, K. Y. & HAMEED, B. 2010. *Insights into Modeling of Adsorption Isotherm Systems*.

GADIPELLY, C., PéREZ-GONZáLEZ, A., YADAV, G. D., ORTIZ, I., IBáñEZ, R., RATHOD, V. K. & MARATHE, K. V. 2014. Pharmaceutical Industry Wastewater: Review of the Technologies for Water Treatment and Reuse. *Industrial & Engineering Chemistry Research,* 53**,** 11571-11592.

GAO, Y., LI, Y., ZHANG, L., HUANG, H., HU, J., SHAH, S. M. & SU, X. 2012. Adsorption and removal of tetracycline antibiotics from aqueous solution by graphene oxide. *Journal of Colloid and Interface Science,* 368**,** 540-546.

HAO, W., BJöRKMAN, E., YUN, Y., LILLIESTRåLE, M. & HEDIN, N. 2014. *Iron Oxide Nanoparticles Embedded in Activated Carbons Prepared from Hydrothermally Treated Waste Biomass*.

HELFFERICH, F. G. 1985. Principles of adsorption & adsorption processes, by D. M. Ruthven, John Wiley & Sons, 1984, xxiv + 433 pp. *AIChE Journal,* 31**,** 523-524.

ISSA, B., OBAIDAT, I. M., ALBISS, B. A. & HAIK, Y. 2013. Magnetic Nanoparticles: Surface Effects and Properties Related to Biomedicine Applications. *International Journal of Molecular Sciences,* 14**,** 21266-21305.

JIN, G., EOM, Y. & LEE, T. G. 2016. Removal of Hg(II) from aquatic environments using activated carbon impregnated with humic acid. *Journal of Industrial and Engineering Chemistry,* 42**,** 46-52.

JING, X.-R., WANG, Y.-Y., LIU, W.-J., WANG, Y.-K. & JIANG, H. 2014. Enhanced adsorption performance of tetracycline in aqueous solutions by methanol-modified biochar. *Chemical Engineering Journal,* 248**,** 168-174.

KANG, J., LIU, H., ZHENG, Y.-M., QU, J. & CHEN, J. P. 2010. Systematic study of synergistic and antagonistic effects on adsorption of tetracycline and copper onto a chitosan. *Journal of Colloid and Interface Science,* 344**,** 117-125.

KHARISSOVA, O. V., DIAS, H. V. R. & KHARISOV, B. I. 2015. Magnetic adsorbents based on micro- and nano-structured materials. *RSC Advances,* 5**,** 6695-6719.

KIM, S., SHIBATA, E., SERGIIENKO, R. & NAKAMURA, T. 2008. Purification and separation of carbon nanocapsules as a magnetic carrier for drug delivery systems. *Carbon,* 46**,** 1523-1529.

KONG, L. & ADIDHARMA, H. 2019. A new adsorption model based on generalized van der Waals partition function for the description of all types of adsorption isotherms. *Chemical Engineering Journal,* 375**,** 122112.

KUMAR SINGH, V. & ANIL KUMAR, E. 2018. Comparative Studies on CO2 Adsorption Isotherms by Solid Adsorbents. *Materials Today: Proceedings,* 5**,** 23033-23042.

LAOPAIBOON, P., THANI, A., LEELAVATCHARAMAS, V. & LAOPAIBOON, L. 2010. Acid hydrolysis of sugarcane bagasse for lactic acid production. *Bioresource Technology,* 101**,** 1036-1043.

LI, X., CAO, W.-C., LIU, Y.-G., ZENG, G.-M., ZENG, W., QIN, L. & LI, T.-T. 2017. Property Variation of Magnetic Mesoporous Carbon Modified by Aminated Hollow Magnetic Nanospheres: Synthesis, Characterization, and Sorption. *ACS Sustainable Chemistry & Engineering,* 5**,** 179-188.

LI, X., WANG, H., SHAO, G., WANG, G. & LU, L. 2019. Low temperature reduction of NO by activated carbons impregnated with Fe based catalysts. *International Journal of Hydrogen Energy*.

LIANG, C., LI, Z. & DAI, S. 2008. Mesoporous Carbon Materials: Synthesis and Modification. *Angewandte Chemie International Edition,* 47**,** 3696-3717.

LIAO, X., LI, B., ZOU, R., DAI, Y., XIE, S. & YUAN, B. 2016. Biodegradation of antibiotic ciprofloxacin: pathways, influential factors, and bacterial community structure. *Environmental Science and Pollution Research,* 23**,** 7911-7918.

LIN, C.-R., CHU, Y.-M. & WANG, S.-C. 2006. Magnetic properties of magnetite nanoparticles prepared by mechanochemical reaction. *Materials Letters,* 60**,** 447-450.

LIN, Y., XU, S. & JIA, L. 2013a. *Fast and highly efficient tetracyclines removal from environmental waters by graphene oxide functionalized magnetic particles*.

LIN, Y., XU, S. & LI, J. 2013b. Fast and highly efficient tetracyclines removal from environmental waters by graphene oxide functionalized magnetic particles. *Chemical Engineering Journal,* 225**,** 679-685.

LIU, P., LIU, W.-J., JIANG, H., CHEN, J.-J., LI, W.-W. & YU, H.-Q. 2012. Modification of bio-char derived from fast pyrolysis of biomass and its application in removal of tetracycline from aqueous solution. *Bioresource Technology,* 121**,** 235-240.

LOFRANO, G., LIBRALATO, G., ADINOLFI, R., SICILIANO, A., IANNECE, P., GUIDA, M., GIUGNI, M., VOLPI GHIRARDINI, A. & CAROTENUTO, M. 2016. Photocatalytic degradation of the antibiotic chloramphenicol and effluent toxicity effects. *Ecotoxicology and Environmental Safety,* 123**,** 65-71.

LOMPE, K. M., VO DUY, S., PELDSZUS, S., SAUVé, S. & BARBEAU, B. 2018. Removal of micropollutants by fresh and colonized magnetic powdered activated carbon. *Journal of Hazardous Materials,* 360**,** 349-355.

MA, H., LI, J.-B., LIU, W.-W., MIAO, M., CHENG, B.-J. & ZHU, S.-W. 2015. Novel synthesis of a versatile magnetic adsorbent derived from corncob for dye removal. *Bioresource Technology,* 190**,** 13-20.

MA, Y., ZHOU, Q., LI, A., SHUANG, C., SHI, Q. & ZHANG, M. 2014. Preparation of a novel magnetic microporous adsorbent and its adsorption behavior of p-nitrophenol and chlorotetracycline. *Journal of Hazardous Materials,* 266**,** 84-93.

MANOCHA, S. M. 2003. Porous carbons. *Sadhana,* 28**,** 335-348.

MARTINS, A. C., PEZOTI, O., CAZETTA, A. L., BEDIN, K. C., YAMAZAKI, D. A. S., BANDOCH, G. F. G., ASEFA, T., VISENTAINER, J. V. & ALMEIDA, V. C. 2015. Removal of tetracycline by NaOH-activated carbon produced from macadamia nut shells: Kinetic and equilibrium studies. *Chemical Engineering Journal,* 260**,** 291-299.

MARZBALI, M. H. & ESMAIELI, M. 2017. Fixed bed adsorption of tetracycline on a mesoporous activated carbon: Experimental study and neuro-fuzzy modeling. *Journal of Applied Research and Technology,* 15**,** 454-463.

MEHTA, D., MAZUMDAR, S. & SINGH, S. K. 2015. Magnetic adsorbents for the treatment of water/wastewater—A review. *Journal of Water Process Engineering,* 7**,** 244-265.

OU, J., MEI, M. & XU, X. 2016. Magnetic adsorbent constructed from the loading of amino functionalized Fe3O4 on coordination complex modified

polyoxometalates nanoparticle and its tetracycline adsorption removal property study. *Journal of Solid State Chemistry,* 238**,** 182-188.

OUBAGARANADIN, J. U. K. & MURTHY, Z. V. P. 2011. *Activated carbons: Classifications, properties and applications*.

OUZZINE, M., ROMERO-ANAYA, A. J., LILLO-RóDENAS, M. A. & LINARES-SOLANO, A. 2019. Spherical activated carbons for the adsorption of a real multicomponent VOC mixture. *Carbon,* 148**,** 214-223.

PANDEY, A., SOCCOL, C. R., NIGAM, P. & SOCCOL, V. T. 2000. Biotechnological potential of agro-industrial residues. I: sugarcane bagasse. *Bioresource Technology,* 74**,** 69-80.

PENG, L., REN, Y., GU, J., QIN, P., ZENG, Q., SHAO, J., LEI, M. & CHAI, L. 2014. Iron improving bio-char derived from microalgae on removal of tetracycline from aqueous system. *Environmental Science and Pollution Research,* 21**,** 7631-7640.

QIAO, M., YING, G.-G., SINGER, A. C. & ZHU, Y.-G. 2018. Review of antibiotic resistance in China and its environment. *Environment International,* 110**,** 160-172.

RAI, P. & SINGH, K. P. 2018. Valorization of Poly (ethylene) terephthalate (PET) wastes into magnetic carbon for adsorption of antibiotic from water: Characterization and application. *Journal of Environmental Management,* 207**,** 249-261.

SANKAR, S., SARAVANAN, S., AHMED, A. T. A., INAMDAR, A. I., IM, H., LEE, S. & KIM, D. Y. 2019. Spherical activated-carbon nanoparticles derived from biomass green tea wastes for anode material of lithium-ion battery. *Materials Letters,* 240**,** 189-192.

SING, K. 2001. The use of nitrogen adsorption for the characterisation of porous materials. *Colloids and Surfaces A: Physicochemical and Engineering Aspects,* 187-188**,** 3-9.

TAO, J., QIN, L., LIU, X., LI, B., CHEN, J., YOU, J., SHEN, Y. & CHEN, X. 2017. Effect of granular activated carbon on the aerobic granulation of sludge and its mechanism. *Bioresource Technology,* 236**,** 60-67.

WANG, Y., WANG, J., MA, C., QIAO, W. & LING, L. 2019. Fabrication of hierarchical carbon nanosheet-based networks for physical and chemical adsorption of CO2. *Journal of Colloid and Interface Science,* 534**,** 72-80.

XIE, A., CUI, J., CHEN, Y., LANG, J., LI, C., YAN, Y. & DAI, J. 2019. Simultaneous activation and magnetization toward facile preparation of auricularia-based magnetic porous carbon for efficient removal of tetracycline. *Journal of Alloys and Compounds,* 784**,** 76-87.

XIE, A., DAI, J., CHEN, X., MA, P., HE, J., LI, C., ZHOU, Z. & YAN, Y. 2016. Ultrahigh adsorption of typical antibiotics onto novel hierarchical porous carbons derived from renewable lignin via halloysite nanotubes-template and in-situ activation. *Chemical Engineering Journal,* 304**,** 609-620.

ZHANG, P., LI, Y., CAO, Y. & HAN, L. 2019. Characteristics of tetracycline adsorption by cow manure biochar prepared at different pyrolysis temperatures. *Bioresource Technology,* 285**,** 121348.

ZHANG, Z., LAN, H., LIU, H. & QU, J. 2015. Removal of tetracycline antibiotics from aqueous solution by amino-Fe (III) functionalized SBA15. *Colloids and Surfaces A: Physicochemical and Engineering Aspects,* 471**,** 133-138.

ZHOU, L., MA, J., ZHANG, H., SHAO, Y. & LI, Y. 2015. Fabrication of magnetic carbon composites from peanut shells and its application as a heterogeneous Fenton catalyst in removal of methylene blue. *Applied Surface Science,* 324**,** 490-498.

ZHOU, L., SHAO, Y., LIU, J., YE, Z., ZHANG, H., MA, J., JIA, Y., GAO, W. & LI, Y. 2014. Preparation and Characterization of Magnetic Porous Carbon Microspheres for Removal of Methylene Blue by a Heterogeneous Fenton Reaction. *ACS Applied Materials & Interfaces,* 6**,** 7275-7285.

ZHOU, Q., LI, Z., SHUANG, C., LI, A., ZHANG, M. & WANG, M. 2012. *Efficient removal of tetracycline by reusable magnetic microspheres with a high surface area*.

ZHU, H. Y., FU, Y. Q., JIANG, R., JIANG, J. H., XIAO, L., ZENG, G. M., ZHAO, S. L. & WANG, Y. 2011. Adsorption removal of congo red onto magnetic cellulose/Fe3O4/activated carbon composite: Equilibrium, kinetic and thermodynamic studies. *Chemical Engineering Journal,* 173**,** 494-502.

ZHU, X., LIU, Y., QIAN, F., ZHOU, C., ZHANG, S. & CHEN, J.-M. 2013. *Preparation of magnetic porous carbon from waste hydrochar by simultaneous activation and magnetization for tetracycline removal*.

ZHU, X., LIU, Y., QIAN, F., ZHOU, C., ZHANG, S. & CHEN, J. 2014a. Preparation of magnetic porous carbon from waste hydrochar by simultaneous activation and magnetization for tetracycline removal. *Bioresource Technology,* 154**,** 209-214.

ZHU, X., LIU, Y., ZHOU, C., LUO, G., ZHANG, S. & CHEN, J. 2014b. A novel porous carbon derived from hydrothermal carbon for efficient adsorption of tetracycline. *Carbon,* 77**,** 627-636.

ZHU, Y., ZHANG, L., SCHAPPACHER, F. M., PöTTGEN, R., SHI, J. & KASKEL, S. 2008. Synthesis of Magnetically Separable Porous Carbon Microspheres and Their Adsorption Properties of Phenol and Nitrobenzene from Aqueous Solution. *The Journal of Physical Chemistry C,* 112**,** 8623-8628.

VITAE

Name Miss Sirinad Mahawong

Student ID 6010220056

Educational Attainment

Degree	Name of Institution	Year of Graduation
Bachelor of Science (Chemistry)	Prince of Songkla University	2016

Scholarship Awards during Enrolment

Science Achievement Scholarship of Thailand (SAST)

List of Publication and Proceeding

Mahawong, S., Saning, A., Watcharin, W., Dechtrirat, D. and Chuenchom, L. 2019. Facile preparation of a magnetic carbon adsorbent via simultaneous magnetization and activation of sugarcane bagasse and Fe^{2+} and Fe^{3+} ions, in Proceeding IOP conference series: materials science and engineering.

Mahawong, S., Dechtrirat, D., Watcharin, W., Wattanasin, P., Muensit, N. and Chuenchom, L. 2019. Mesoporous Magnetic Carbon Adsorbents Prepared from Sugarcane Bagasse and Fe^{2+} and Fe^{3+} via Simultaneous Magnetization and Activation for Tetracycline Adsorption. *Science of Advanced Materials*, 11, 1-12.

KAEOBAMRUNG, J., LANUI, A., MAHAWONG, S., DUANGMAK, W. & RUKACHAISIRIKUL, V. 2015. One-pot synthesis of trisubstituted ureas from α-chloroaldoxime O-methanesulfonates and secondary amines. RSC Advances, 5, 58587-58594.

List of Presentation

Mahawong, S., Saning, A., Watcharin, W., Dechtrirat, D. and Chuenchom, L. 2018. Facile preparation of a magnetic carbon adsorbent via simultaneous magnetization and activation of sugarcane bagasse and Fe^{2+} and Fe^{3+} ions, International Conference on Materials Research and Innovation (ICMARI).

Mahawong, S., Dechtrirat, D., Watcharin, W., Wattanasin, P., Muensit, N. and Chuenchom. 2019. Mesoporous Magnetic Carbon Adsorbents Prepared from Sugarcane Bagasse and Fe^{2+} and Fe^{3+} via Simultaneous Magnetization and Activation for Tetracycline Adsorption, The 2019 Pure and Applied Chemistry International Conference (PACCON 2019), p. 141.